Available online at www.sciencedirect.com
SCIENCE DIRECT®
ELSEVIER
International Journal of Solids and Structures 43 (2006) 523–550
INTERNATIONAL JOURNAL OF SOLIDS and STRUCTURES
www.elsevier.com/locate/ijsolstr

On the longitudinal impact of two phase transforming bars. Elastic versus a rate-type approach. Part II: The rate-type case

Cristian Făciu [a,*], Alain Molinari [b]

[a] *Institute of Mathematics of the Romanian Academy, P.O. Box 1-764, RO-014700 Bucharest, Romania*
[b] *Laboratoire de Physique et Mécanique des Matériaux, U.M.R.—C.N.R.S. 7554, Université de Metz, Ile du Saulcy, F-57045 Metz, France*

Received 20 September 2004; received in revised form 6 June 2005
Available online 2 August 2005

Abstract

We study the propagation of phase transformation fronts induced by the longitudinal impact of two shape memory alloy bars modeled by a general form of a rate-type approach to non-monotone elasticity. We illustrate that such a rate-type law should be seen like a kinetic law for phase transformation. This investigation continues in a comparative way the analysis of the dynamic theory of elastic bar considered in Part I in relation with a viscosity criterion. We focus here on mathematical, thermodynamical and experimental aspects related with the wave structure which accompanies both the forward and reverse transformation. We analyze the propagation of disturbances in a pure phase near and far from their sources, that is the instantaneous waves and the delayed waves as well as the traveling wave solutions and the accompanying dissipation. In the numerical experiments one focuses on the influence of the impact velocity on the way the phase boundary propagates and on the results which can indicate indirectly the existence of a phase transformation like the time of separation, the velocity–time profile at the rear end of the target and the stress history at the impact face.

Keywords: Phase transition; Kinetic law; Bar impact; Perturbation; Shape memory alloys

* Corresponding author. Fax: +4021 319 65 05.
E-mail address: cristian.faciu@imar.ro (C. Făciu).

0020-7683/$ - see front matter © 2005 Elsevier Ltd. All rights reserved.
doi:10.1016/j.ijsolstr.2005.06.022

1. Introduction

The first part of this paper (Făciu and Molinari, 2005) has been concerned with the dynamic analysis of impact-induced phase transitions in elastic phase transforming bars, with a special focus on the admissible wave structure corresponding to a viscosity criterion, equivalent with the well-known chord criterion. Such elasto-dynamical aspects of the nucleation phenomena are connected, for instance, with the papers by James (1980), Slemrod (1983), Pego (1987). The exact solution obtained for dynamic interactions of elastic shock waves and phase transformation fronts for a non-monotone piecewise linear stress–strain relation has been used in Part I to investigate the longitudinal impact of bars as a controlled mean for inducing the transformation.

In this paper, we study the same longitudinal impact problem for thin bars of phase transforming materials, like shape memory alloys, by using an augmented general rate-type theory. The outline of this paper is as follows.

In Section 2, we introduce our constitutive assumptions. We consider a general form of a Maxwellian rate-type constitutive equation whose equilibrium is described by an elastic non-monotone stress–strain relation. This equation, which includes viscosity μ, a rate sensitivity parameter λ and a dynamic Young modulus E, can describe the way the body may deviate from equilibrium, therefore the kinetics of transformation. We show that the proposed rate-type law possesses its own kinetics due to the dissipative viscous mechanism incorporated without the need of a separate nucleation criterion and we identify the material parameters which characterize the rate at which the material transforms. Thus, this constitutive equation should be seen as a kinetic law for phase transitions in phase transforming bars.

Such kind of constitutive relation has been successfully used, for instance by Suliciu (1992), Făciu and Suliciu (1994) and Făciu (1996), to describe instabilities which accompany phase transformation phenomena during quasistatic strain- and stress-controlled experiments. By taking into account the dependence on temperature of the equilibrium stress–strain relation, this isothermal rate-type model has been extended by Făciu and Mihăilescu-Suliciu (2002) in order to include thermal effects associated with phase transitions in shape memory alloy bars and its predictions have been found in very good agreement with the experiments done by Shaw and Kyriakides (1997).

Let us note that our rate-type approach contains as a special case the well known Kelvin–Voigt viscosity model which is obtained by simply making the dynamic Young modulus to go to infinite in our constitutive relation. This regularized model has been used by Pego (1987), Vainchtein and Rosakis (1999) and Vainchtein (2002) to describe phase transformation in solid bars.

In Section 3 we discuss the compatibility of our constitutive approach with the second law of thermodynamics and we focus on the corresponding internal dissipation. We deduce some energetic identities and inequalities. The free energy of the Kelvin–Voigt model and all its energetic properties are deduced by simply making the dynamic Young modulus $E \to \infty$. We show that both models approximate the equilibrium curve in an $L^{\lambda+1}$ sense when the viscosity $\mu \to 0$. Moreover, by using the properties of the free energy function, we show that the moving strain discontinuities of the Maxwellian rate-type system, which coincide with the characteristic directions of the hyperbolic semilinear system, *are not dissipative*.

In Section 4, by studying traveling wave solutions for the Maxwellian's type system, we deduce a viscosity criterion for the admissibility of weak solutions for the elastic system. This criterion is equivalent with the chord criterion, that is, the same selection criterion as for Kelvin–Voigt's materials (see Pego, 1987). It is known that a phase transformation process is strongly dissipative. The question is in which way this dissipation appears? The answer is given by investigating the total internal dissipation corresponding to a traveling wave which describes a smooth phase transition in the rate-type theory. We get that this is just the dissipation induced by an admissible sharp phase transition in the elastic theory. That means, the dissipation of a traveling wave does not depend on the kinetic parameters: viscosity μ, rate sensitivity parameter λ

and dynamic young modulus E. These kinetic parameters influence only the smooth transition layer which approximate a sharp interface.

In Section 5 we investigate, following Brun and Molinari (1982), by using the method of multiple scales, the propagation of disturbances in a pure phase, near and far from their sources. We want to know which set of waves are the most important and will really be observed and to determine the speeds at which the disturbances travel and the way they promote dissipation. Our analysis leads to two kind of waves: instantaneous waves and delayed waves. We establish that near the source the waves propagate with the speeds $\pm\sqrt{E/\varrho}$ (*instantaneous waves*) being immediately exponentially damped. On the other hand, in the unstable phases any inhomogeneity in the strain or stress fields lead to the nucleation and, consequently to the formation of a *stationary phase boundary*. Far from the source, the main part of the disturbance moves with the slower speeds $\pm\sqrt{E_0/\varrho}$ (*delayed waves*), where E_0 is the elastic modulus of the equilibrium (elastic) curve in a stable phase. The amplitude of the disturbances far from their source decreases like $1/\sqrt{at}$, which is typical for diffusion and spreads out like $\sqrt{at}$ where a is a diffusion coefficient proportional with μ (see also Whitham, 1959). Since the strain discontinuities for the Maxwellian's rate-type system, propagating along the characteristic lines, are not dissipative, the behavior of the delayed waves which propagate through a diffusion process characterizes in fact the dissipative nature of the rate-type approach in a pure phase. Since the occurrence of diffusion is not envisaged in phase transition phenomena in shape memory bars, the benefit of this investigation is that it suggests how to choose the new material parameters of the rate-type model (E and μ) in order to avoid diffusivity phenomena introduced by the rate-type terms. This analysis also illustrates the advantages in using the Maxwell's type approach to describe the propagation of disturbances in phase transforming materials with respect to the Kelvin–Voigt's approach.

In Section 6 we investigate numerically the longitudinal impact of two phase transforming bars for material parameters appropriate for a NiTi shape memory alloy. One aim of this study is to compare the exact solution obtained using the elastic model with the numerical solution obtained by using the Maxwellian's rate-type model. A very good agreement is found. We focus on those numerical results which can be determined experimentally: the velocity at the free end of the target bar, the time of separation between the two bars after impact and the stress history at the impact face. We also insist on the differences between the predictions of the two models and we discuss the advantages provided by the rate-type approach. These numerical results are qualitatively in agreement with the experimental measurements performed by Escobar and Clifton (1995). A work aiming to correlate the model predictions with future experimental results is necessary.

2. A general rate-type approach to phase transitions

We consider in the following, the system of PDEqs governing the longitudinal motion of a thin bar, which can support a phase transformation, described by a Maxwell's rate-type constitutive equation

$$\varrho\frac{\partial v}{\partial t}-\frac{\partial \sigma}{\partial X}=0,\quad \frac{\partial \varepsilon}{\partial t}-\frac{\partial v}{\partial X}=0, \tag{1}$$

$$\frac{\partial \sigma}{\partial t}-E\frac{\partial \varepsilon}{\partial t}=-\frac{E}{\mu}\left|\sigma-\sigma_{\mathrm{eq}}(\varepsilon)\right|^{\lambda-1}(\sigma-\sigma_{\mathrm{eq}}(\varepsilon)), \tag{2}$$

where $t>0$ is time, X is the spatial coordinate along the bar, v is the particle velocity, ε is the strain, σ is the stress and $\varrho=\text{const.}>0$ is the mass density in a reference configuration which corresponds to a defined phase of the material.

$E=\text{const.}>0$ is the *dynamic Young modulus*, $\lambda=\text{const.}>0$ is a *rate sensitivity parameter* and $\mu=\text{const.}>0$ is a *viscosity coefficient*. For $\lambda=1$, μ is a *Newtonian viscosity coefficient*, $\frac{\mu}{E}$ is a *relaxation time*

of the model, while $k = \frac{E}{\mu}$ is usually called *Maxwellian viscosity coefficient*. When $\mu \to 0$ this rate-type constitutive equation, can be seen as a rate-type approach of the elastic model in a sense which will be presented latter. From physical point of view it introduces a mechanism of energy dissipation of kinetic origin modeled by a Maxwell-type viscosity.

In order to describe phase transition phenomena we suppose that

$$\sigma = \sigma_{\mathrm{eq}}(\varepsilon), \tag{3}$$

called the *equilibrium curve*, is a *non-monotone* stress–strain relation which for the present purposes is taken piecewise linear, i.e. (see Fig. (3.1) in Part I)

$$\sigma = \sigma_{\mathrm{eq}}(\varepsilon) = \begin{cases} E_3\varepsilon - \sigma_3, & \text{for } \varepsilon_{\mathrm{m}} \leqslant \varepsilon, \\ -E_2\varepsilon + \sigma_2, & \text{for } \varepsilon_{\mathrm{a}} < \varepsilon < \varepsilon_{\mathrm{m}}, \\ E_1\varepsilon, & \text{for } -\varepsilon_{\mathrm{a}} \leqslant \varepsilon \leqslant \varepsilon_{\mathrm{a}}, \\ -E_2\varepsilon - \sigma_2, & \text{for } -\varepsilon_{\mathrm{m}} < \varepsilon < -\varepsilon_{\mathrm{a}}, \\ E_3\varepsilon + \sigma_3, & \text{for } \varepsilon \leqslant -\varepsilon_{\mathrm{m}}, \end{cases} \tag{4}$$

where $\sigma_2 = (E_1 + E_2)\varepsilon_{\mathrm{a}} > 0$, $\sigma_3 = (E_3 + E_2)\varepsilon_{\mathrm{m}} - (E_1 + E_2)\varepsilon_{\mathrm{a}} = E_3\varepsilon_{\mathrm{m}} - \sigma_{\mathrm{m}}$ and $0 < \varepsilon_{\mathrm{a}} < \varepsilon_{\mathrm{m}}$.

We denote by

$$\sigma_{\mathrm{a}} = E_1\varepsilon_{\mathrm{a}} > 0 \quad \text{and} \quad \sigma_{\mathrm{m}} = -E_2(\varepsilon_{\mathrm{m}} - \varepsilon_{\mathrm{a}}) + E_1\varepsilon_{\mathrm{a}},$$

the values of tensile stresses where the monotony of the equilibrium stress–strain relation changes.

This constitutive relation is viewed as corresponding to a material which can exist in an *austenite phase* $(\mathscr{A})(X \in \mathscr{A} \Longleftrightarrow \varepsilon(X) \in [-\varepsilon_{\mathrm{a}}, \varepsilon_{\mathrm{a}}])$ and in two *variants of martensite* $(\mathscr{M}^{\pm})(X \in \mathscr{M}^{-} \Longleftrightarrow \varepsilon(X) \leqslant -\varepsilon_{\mathrm{m}}$ and $X \in \mathscr{M}^{+} \Longleftrightarrow \varepsilon(X) \geqslant \varepsilon_{\mathrm{m}})$. $E_1 = \text{const.} > 0$ is called the elastic modulus of the austenite phase, while $E_3 = \text{const.} > 0$ is the elastic modulus of the martensite phase since the variants of martensite are crystallographically equivalent. $-E_2 = \text{const.} < 0$ is called the softening modulus and it corresponds to the *unstable phases* of the material $\mathscr{I}^{-} \cup I^{+} \equiv (-\varepsilon_{\mathrm{m}}, -\varepsilon_{\mathrm{a}}) \cup (\varepsilon_{\mathrm{a}}, \varepsilon_{\mathrm{m}})$.

The first constitutive equation of type (2) with the right hand side equal to $-\sigma$ has been proposed by Maxwell in 1867 and this explains why materials described by such relations are often called Maxwellian materials. Let us note that for $\lambda = 1$ the constitutive equation (2) reduces to the *Maxwell's rate-type constitutive equation* used by Suliciu (1992), Făciu and Suliciu (1994), Făciu (1996) to describe the hysteretic behavior in strain- or stress-controlled experiments as well as the nucleation and growth/decay of phases. The case $\lambda \neq 1$ has also been considered by Făciu (1991) when investigating phase transitions in rate-type fluids with relaxation of van der Waals type. Rate-type constitutive equations with over-stress power law of type (2) have been considered in dynamic plasticity by Kukudjanov (1967) and Suliciu et al. (1972).

From mathematical point of view, the rate-type system (1) and (2) has the advantage that it is always *hyperbolic semilinear* as long as the dynamic Young's modulus E is strictly positive and finite. The characteristic directions of this system are given by

$$\frac{\mathrm{d}X}{\mathrm{d}t} = \pm\sqrt{\frac{E}{\varrho}} \quad \text{and} \quad \frac{\mathrm{d}X}{\mathrm{d}t} = 0. \tag{5}$$

The initial-boundary value problems are now well-posed even in the spinodal regions $\mathscr{I}^{\pm}$. It was shown for the case $\lambda = 1$ (Suliciu, 1992; Făciu, 1996) that the rate-type system incorporates some physical instabilities due to the shape of the equilibrium curve and it is able to describe general issues pertaining to phase transition phenomena.

From mechanical point of view, unlike the elastic model, the constitutive equation (2) can describe the way the body may deviate from equilibrium. Indeed, this model has the capability to describe instantaneous, relaxation and pseudo-creep processes.

We remind that an *instantaneous process* relative to a given state $(\varepsilon_0, \sigma_0)$ is the solution $\varepsilon \to \sigma_I(\varepsilon)$ of the differential equation

$$\frac{d\sigma_I(\varepsilon)}{d\varepsilon} = E, \quad \sigma_I(\varepsilon_0) = \sigma_0. \tag{6}$$

We also note that the equilibrium curve is attractive for any *relaxation process* $(\varepsilon(t) = \varepsilon_0 = \text{const.}, \sigma(t))$, $t > 0$, where

$$\dot{\sigma}(t) = -\frac{E}{\mu}|\sigma - \sigma_{eq}(\varepsilon_0)|^{\lambda-1}(\sigma - \sigma_{eq}(\varepsilon_0)), \quad \sigma(0) = \sigma_0. \tag{7}$$

Indeed, one easily verifies that any relaxation process starting at a state $(\varepsilon_0, \sigma_0)$ ends on the equilibrium curve after a *finite* time interval for $\lambda \in (0,1)$ and an *infinite* time interval for $\lambda \in [1, \infty)$.

The equilibrium states $(\varepsilon, \sigma_{eq}(\varepsilon))$ of the constitutive equation (2) are called *stable/unstable* if $\frac{d\sigma_{eq}(\varepsilon)}{d\varepsilon} \geqslant 0 \Big/ \frac{d\sigma_{eq}(\varepsilon)}{d\varepsilon} < 0$. One mechanical reason to use this terminology is due to the fact that the equilibrium curve $\sigma_{eq}(\varepsilon)$ is *attractive/repulsive* for any *pseudo-creep process* $(\varepsilon = \varepsilon(t),\ \sigma(t) = \sigma_0 = \text{const.})$ starting at a state $(\varepsilon_0, \sigma_0)$, when $\frac{d\sigma_{eq}(\varepsilon_0)}{d\varepsilon} > 0 \Big/ \frac{d\sigma_{eq}(\varepsilon_0)}{d\varepsilon} < 0$. Therefore, any solution of the problem

$$\dot{\varepsilon}(t) = \frac{1}{\mu}|\sigma_0 - \sigma_{eq}(\varepsilon)|^{\lambda-1}(\sigma_0 - \sigma_{eq}(\varepsilon)), \quad \varepsilon(0) = \varepsilon_0. \tag{8}$$

ends always on the stable parts of the equilibrium curve.

The rate-type constitutive relation (2) includes as a limiting case for $E \to \infty$ the following generalized *Kelvin–Voigt viscoelastic model*

$$\dot{\varepsilon}(t) = \frac{1}{\mu}|\sigma - \sigma_{eq}(\varepsilon)|^{\lambda-1}(\sigma - \sigma_{eq}(\varepsilon)), \tag{9}$$

or, equivalently

$$\sigma = \sigma_{eq}(\varepsilon) + \mu^m|\dot{\varepsilon}|^{m-1}\dot{\varepsilon}, \tag{10}$$

where $m = 1/\lambda$.

For $m = 1$, this equation has been considered by James (1980), latter by Pego (1987) and recently by Vainchtein and Rosakis (1999) in relation with phase transformations in solids.

Let us note that Kelvin–Voigt's viscoelastic constitutive equation can describe only pseudo-creep processes which are governed by the same Eq. (8), while any instantaneous process has an infinite slope. The field equation system (1) and (9) is now *parabolic* and any Cauchy problem is also well-posed in the sense of Hadamard. Indeed, if we look at the Kelvin–Voigt viscoelastic system (1) and (9) as a limiting case of the system (1) and (2) for $E \to \infty$, we observe by using relations (5) that the characteristic directions of the system in the $t-X$ plane tends to infinite, i.e. the hyperbolic system (1) and (2) transforms into the parabolic one (1) and (10).

It is well-known that, as an alternative approach to describing phenomenologically the kinetics of growth of phases, one can directly regularize the elastic model and obtain an admissibility condition for the propagating fronts. There are several alternative regularization schemes including different variants of visco-elasticity and gradient elasticity (see for instance Ngan and Truskinovsky (2002) and the literature therein). Sometimes such models, like our rate-type constitutive equation (2) for example, are only considered as a mathematical regularization of the elastic model (3) and not like a physical model for the kinetics of phase transformations and therefore viewed with suspicion. One reason is due to the fact that the viscous properties of phase transforming materials, like shape memory alloys for instance, are not important. Therefore the *viscoelastic* denomination of this law seems to be inappropriate in this context. In fact, the role of the internal dissipation of kinetic origin modeled by a viscous approach is essential only in

the transition unstable zones. Consequently, it is better to regard (2) from a physical point of view as a *kinetic law* for phase transformations and we illustrate in the following by simple examples the way the transformation proceeds. In Section 5, we also explain analytically how the non-equilibrium evolution of the particles of the bar towards stable phases appears without the need of a separate nucleation criterion.

Let us consider, for example, an initial state $(\varepsilon_0 = \varepsilon^* + \eta, \sigma_0 = \sigma_{eq}(\varepsilon^*))$, $\eta > 0$ as a perturbation of an equilibrium state $(\varepsilon^*, \sigma^* = -E_2\varepsilon^* + \sigma_2)$ in the unstable phase $\mathscr{I}^+$ of the material. If we investigate pseudo-creep processes $(\varepsilon = \varepsilon(t), \sigma(t) = \sigma_0)$, as solution of (8) when $\sigma_{eq}(\varepsilon)$ is given by (4), we can explore how the strain evolves towards stable phases, that is the rate at which the material transforms from one phase to another. We get the following relations:

- for $\lambda = 1$

$$\varepsilon(t) = \begin{cases} \varepsilon^* + \eta \exp\left(\frac{E_2}{\mu} t\right), & t \in [0, t_m), \\ \varepsilon^* + (\varepsilon_m - \varepsilon^*)\left(1 + \frac{E_2}{E_3}\right) - \frac{E_2}{E_3}(\varepsilon_m - \varepsilon^*) \exp\left(\frac{-E_3}{\mu}(t - t_m)\right), & t \in [t_m, \infty), \end{cases} \tag{11}$$

where $t_m = \frac{\mu}{E_2} \ln \frac{(\varepsilon_m - \varepsilon^*)}{\eta}$,

- for $\lambda \neq 1$

$$\varepsilon(t) = \begin{cases} \varepsilon^* + \left[\eta^{1-\lambda} + \frac{E_2^{\lambda}(1-\lambda)}{\mu} t\right]^{\frac{1}{1-\lambda}}, & t \in [0, t_m), \\ \varepsilon^* + (\varepsilon_m - \varepsilon^*)\left(1 + \frac{E_2}{E_3}\right) - \left[\left(\frac{E_2}{E_3}(\varepsilon_m - \varepsilon^*)\right)^{1-\lambda} - \frac{E_3^{\lambda}(1-\lambda)}{\mu}(t - t_m)\right]^{\frac{1}{1-\lambda}}, & t \in [t_m, t_f), \end{cases} \tag{12}$$

where $t_m = \frac{\mu}{(1-\lambda)E_2^{\lambda}}[(\varepsilon_m - \varepsilon^*)^{1-\lambda} - \eta^{1-\lambda}]$. For $\lambda > 1$, $t_f = \infty$ while for $\lambda \in (0,1)$ we have $t_f = t_m + \frac{\mu}{(1-\lambda)} \frac{E_2^{1-\lambda}}{E_3}[(\varepsilon_m - \varepsilon^*)]^{1-\lambda}$.

It is obvious that the strain history of a particle, that is, its evolution from a low-phase to a high-phase is controlled by the material parameters μ and λ, which appear in the rate-type model, and by the slopes $-E_2$ and E_3 of the elastic curve. In the examples in Fig. 1 we have considered the perturbation of the equilibrium state $(\varepsilon_a, \sigma_a)$, which is the point where the equilibrium curve $\sigma_{eq}(\varepsilon)$ given by (4) changes the monotony. We have illustrated the way the strain blows up, after entering in the unstable phase $\mathscr{I}^+ = (0.05, 0.065)$, followed by its localization in the phase $\mathscr{M}^+ = (0.065, \infty)$ for different values of μ and λ. We observe in

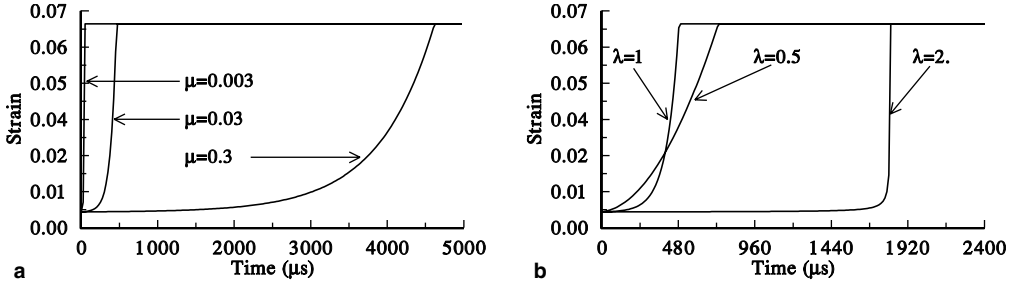

Fig. 1. Kinetics of phase transformation according to Eqs. (11) and (12). Pseudo-creep processes starting at the state $(\varepsilon^* = \varepsilon_a + \eta, \sigma^* = \sigma_a)$ for the numerical entries: $\eta = 0.0001$, $(\varepsilon_a = 0.005, \sigma_a = 150$ MPa), $(\varepsilon_m = 0.065, \sigma_m = 125$ MPa), $E = 31.5$ GPa, $E_1 = E_3 = 30$ GPa, $E_2 = -416.6$ MPa. (a) Influence of the viscosity coefficient μ[MPa s] for $\lambda = 1$. (b) Influence of the rate sensitivity parameter λ for constant $\mu = 0.03$ MPa$^{\lambda}$ s.

Fig. 1a, that when μ decreases, the rate at which the material transforms increases, while the transition time, that is, the time necessary to reach a stable configuration, decreases. On the other side, we observe in Fig. 1b, that when λ increases, there is a waiting time which increases before the instability starts to develop, but once it starts the transformation proceeds faster.

These simple examples suggest that kinetic aspects of phase transformation, which are described by our rate-type approach, should be connected with the time of growth, or time of nucleation of microscopic theories of phase transitions.

3. Energy

If one investigates the compatibility of the rate-type constitutive equation (2) with the second law of thermodynamics, $\varrho\dot{\psi} \leqslant \sigma\dot{\varepsilon}$, where ψ is the Helmholtz free energy, one derives the following results (see Făciu and Mihăilescu-Suliciu, 1987). The constitutive equation (2) admits a unique (modulo a constant) free energy function ψ depending on stress and strain if and only if the slope of the straight line connecting any two points on the equilibrium curve is bounded from above by the instantaneous Young modulus E. Therefore, the elastic moduli of the stable phases in Eq. (4), E_1 and E_3 have to be lower than E. In what follows we suppose there are two positive constants E_* and E^* such that

$$-E_* \leqslant \frac{\sigma_{\mathrm{eq}}(\varepsilon_1) - \sigma_{\mathrm{eq}}(\varepsilon_2)}{\varepsilon_1 - \varepsilon_2} \leqslant E^* < E, \quad \text{for any } \varepsilon_1, \varepsilon_2 \in (-1, \infty), \ \ \varepsilon_1 \neq \varepsilon_2. \tag{13}$$

The free energy function has to satisfy the equation

$$\frac{\partial \psi}{\partial \varepsilon} + E\frac{\partial \psi}{\partial \sigma} = \frac{\sigma}{\varrho}, \quad \psi(0,0) = 0, \tag{14}$$

and the dissipation inequality

$$D_{\mathrm{Mxw}}(\varepsilon, \sigma) \equiv \frac{E}{\mu}\varrho\frac{\partial \psi}{\partial \sigma}(\varepsilon, \sigma)|\sigma - \sigma_{\mathrm{eq}}(\varepsilon)|^{\lambda-1}(\sigma - \sigma_{\mathrm{eq}}(\varepsilon)) \geqslant 0. \tag{15}$$

Therefore, the general form of the free energy function is

$$\varrho\psi(\varepsilon, \sigma) = \frac{\sigma_2}{2E} + \varphi(\sigma - E\varepsilon). \tag{16}$$

Let us denote $h(\varepsilon) \equiv \sigma_{\mathrm{eq}}(\varepsilon) - E\varepsilon$. According to condition (13) function $h = h(\varepsilon)$ is invertible. Therefore, for any pair (ε, σ) there is a unique $\tilde{\varepsilon}$ such that

$$\sigma - E\varepsilon = h(\tilde{\varepsilon}) = \sigma_{\mathrm{eq}}(\tilde{\varepsilon}) - E\tilde{\varepsilon}. \tag{17}$$

One shows finally that the free energy function of the constitutive equation (2) is explicitly determined by the equilibrium curve $\sigma = \sigma_{\mathrm{eq}}(\varepsilon)$ and the Young modulus E through relation

$$\varrho\psi(\varepsilon, \sigma) = \frac{\sigma^2}{2E} - \frac{\sigma_{\mathrm{eq}}^2(\tilde{\varepsilon})}{2E} + \int_0^{\tilde{\varepsilon}} \sigma_{\mathrm{eq}}(s)\,\mathrm{d}s, \tag{18}$$

where $\tilde{\varepsilon} = h^{-1}(\sigma - E\varepsilon)$, h^{-1} being the inverse function of h. Moreover, one can show that the following two relations hold

$$\varrho E\frac{\partial \psi}{\partial \sigma}(\varepsilon, \sigma) = \sigma - \sigma_{\mathrm{eq}}(\tilde{\varepsilon}) = E(\varepsilon - \tilde{\varepsilon}) = E(\varepsilon - h^{-1}(\sigma - E\varepsilon)), \tag{19}$$

$$\frac{E}{E + E_*}(\sigma - \sigma_{\mathrm{eq}}(\varepsilon))^2 \leqslant \varrho E\frac{\partial \psi}{\partial \sigma}(\varepsilon, \sigma)(\sigma - \sigma_{\mathrm{eq}}(\varepsilon)) \leqslant \frac{E}{E - E^*}(\sigma - \sigma_{\mathrm{eq}}(\varepsilon))^2. \tag{20}$$

Thus, from (15) one gets the following estimate on the internal dissipation associated with the Maxwell's type model

$$\frac{E}{\mu(E+E_*)}|\sigma-\sigma_{\rm eq}(\varepsilon)|^{\lambda+1}\leqslant D_{\rm Mxw}(\varepsilon,\sigma)\leqslant\frac{E}{\mu(E-E^*)}|\sigma-\sigma_{\rm eq}(\varepsilon)|^{\lambda+1}. \tag{21}$$

Let us note that if we denote the free energy at equilibrium by $\psi_{\rm eq}(\varepsilon)=\psi(\varepsilon,\sigma_{\rm eq}(\varepsilon))$ we find the classical thermostatic relation $\frac{{\rm d}\psi_{\rm eq}(\varepsilon)}{{\rm d}\varepsilon}=\frac{1}{\varrho}\sigma_{\rm eq}(\varepsilon)$. Therefore, the equilibrium free energy of the Maxwell's type model is just the free energy of the associated elastic model.

If we investigate now the properties of the free energy function $\psi=\psi(\varepsilon,\sigma)$ when $E\to\infty$, we recover the free energy of the generalized Kelvin–Voigt's model (10) which is just the free energy of the associated elastic model. Indeed, from relations (16) and (18) we get

$$\lim_{E\to\infty}\varrho\psi(\varepsilon,\sigma)=\varrho\psi_{\rm eq}(\varepsilon)=\int_0^{\varepsilon}\sigma_{\rm eq}(s)\,{\rm d}s. \tag{22}$$

From (15) and (21) we obtain the internal dissipation associated with the Kelvin–Voigt's model

$$D_{\rm KV}(\varepsilon,\sigma)=\lim_{E\to\infty}D_{\rm Mxw}(\varepsilon,\sigma)=\frac{1}{\mu}(\sigma-\sigma_{\rm eq}(\varepsilon))^{\lambda+1}=\mu^m|\dot\varepsilon|^{m+1}. \tag{23}$$

By using (1), (2) and (14) we can establish the following energy identities for the smooth solutions of the Maxwell's type system (1) + (2)

$$\frac{\partial}{\partial t}\left(\varrho\frac{v^2}{2}+\psi(\varepsilon,\sigma)\right)=\frac{\partial}{\partial X}(\sigma v)-\frac{E}{\mu}\varrho\frac{\partial\psi}{\partial\sigma}|\sigma-\sigma_{\rm eq}(\varepsilon)|^{\lambda-1}(\sigma-\sigma_{\rm eq}(\varepsilon)), \tag{24}$$

and for the Kelvin–Voigt's system (1) + (10)

$$\frac{\partial}{\partial t}\left(\varrho\frac{v^2}{2}+\psi_{\rm eq}(\varepsilon)\right)=\frac{\partial}{\partial X}(\sigma v)-\frac{1}{\mu}|\sigma-\sigma_{\rm eq}(\varepsilon)|^{\lambda+1}, \tag{25}$$

respectively.

Let us denote the total energy of a rate-type bar of length L of Maxwell's type and Kelvin–Voigt's type, respectively by

$$e_{\rm Mxw}(t)=\int_0^L\left(\varrho\frac{v^2}{2}+\psi(\varepsilon,\sigma)\right)(X,t)\,{\rm d}X,\quad\text{and}\quad e_{\rm KV}(t)=\int_0^L\left(\varrho\frac{v^2}{2}+\psi_{\rm eq}(\varepsilon)\right)(X,t)\,{\rm d}X. \tag{26}$$

Then the smooth solutions of the Maxwell's type system (1) + (2) satisfy the energy identity

$$\frac{{\rm d}e_{\rm Mxw}(t)}{{\rm d}t}=-\frac{E}{\mu}\int_0^L\varrho\frac{\partial\psi}{\partial\sigma}|\sigma-\sigma_{\rm eq}(\varepsilon)|^{\lambda-1}(\sigma-\sigma_{\rm eq}(\varepsilon))\,{\rm d}X+(\sigma v)(L,t)-(\sigma v)(0,t), \tag{27}$$

while the smooth solutions of the Kelvin–Voigt's system (1) + (10) satisfy the energy identity

$$\frac{{\rm d}e_{\rm KV}(t)}{{\rm d}t}=-\frac{1}{\mu}\int_0^L|\sigma-\sigma_{\rm eq}(\varepsilon)|^{\lambda+1}\,{\rm d}X+(\sigma v)(L,t)-(\sigma v)(0,t). \tag{28}$$

If we consider now an isolated body problem, i.e. a boundary value problem for which

$$(\sigma v)(L,t)=0\quad\text{and}\quad(\sigma v)(0,t)=0, \tag{29}$$

then from (27) and (28) we derive the following inequalities

$$\frac{{\rm d}e_{\rm Mxw}(t)}{{\rm d}t}\leqslant 0\quad\text{and}\quad\frac{{\rm d}e_{\rm KV}(t)}{{\rm d}t}\leqslant 0. \tag{30}$$

Therefore, for an isolated body problem the total energy of a rate-type bar is a non-increasing function of time. Moreover, by integrating (27) and (28) with respect to the time t and using also the inequalities (20) one gets the following estimates for the solution of the Maxwell's type system (1) + (2)

$$\int_0^t\int_0^L |\sigma-\sigma_{\rm eq}(\varepsilon)|^{\lambda+1} \leqslant \mu\frac{E-E^*}{E}(e_{\rm Mxw}(0)-e_{\rm Mxw}(t)) \leqslant \mu\frac{E-E^*}{E}e_{\rm Mxw}(0), \tag{31}$$

and for the solution of the Kelvin–Voigt's system (1) + (10)

$$\int_0^t\int_0^L |\sigma-\sigma_{\rm eq}(\varepsilon)|^{\lambda+1} \leqslant \mu(e_{\rm KV}(0)-e_{\rm KV}(t)) \leqslant \mu e_{\rm KV}(0). \tag{32}$$

Therefore, for both rate-type models we have an approach of the equilibrium curve $\sigma=\sigma_{\rm eq}(\varepsilon)$ in $L^{\lambda+1}$ sense when $\mu\to 0$.

Let us note that Kelvin–Voigt's system can not describe sharp propagating strain discontinuities since it is a parabolic one. On the other side, Maxwell's rate-type system (1) and (2) is hyperbolic semilinear and the characteristics (5) act as transporters of the discontinuities of v, ε and σ and of its partial derivatives. In other words, the shock waves and acceleration waves lie between the characteristic directions of the system. Moreover, *the strain discontinuities of the Maxwell's rate-type system, propagating with the speed* $\dot S=\pm\sqrt{E/\varrho}$, *are not dissipative*.

Indeed, let us remember that the dissipation inequality for a strain discontinuity is $D=\dot S(t)(\varrho[\psi]-[\varepsilon](\sigma^++\sigma^-)/2)\geqslant 0$. According to (6), if the strain jumps in time at a state (ε^-,σ^-) from ε^- to ε^+ then the corresponding stress σ^+ is obtained as $\sigma^+=\sigma_{\rm I}(\varepsilon^+)=E(\varepsilon^+-\varepsilon^-)+\sigma^-$. Therefore, across any propagating strain discontinuity we have $[\sigma]=E[\varepsilon]$. By using the expression (16) of the free energy function for Maxwell's type constitutive equation (2) we get

$$D=\dot S\left(\frac{(\sigma^+)^2-(\sigma^-)^2}{2E}+\varphi(\sigma^+-E\varepsilon^+)-\varphi(\sigma^--E\varepsilon^-)-\frac{\sigma^++\sigma^-}{2}(\varepsilon^+-\varepsilon^-)\right)=0. \tag{33}$$

4. Traveling waves, chord criterion and dissipation

By considering an augmented theory for the non-monotone elastic model, as the Maxwellian rate-type approach (2) is, one introduces in fact a dissipative viscous mechanism of kinetic origin inside the phase transition front. That means, one introduces an internal structure in a transition layer of finite thickness which replaces a sharp phase boundary. Moreover, in the limit in which this viscous added effect vanishes the elastic wave structure with sharp interfaces inherits the wave structure of the augmented theory.

Therefore, in the following we use a standard procedure to establish a criterion to identify admissible phase boundaries within the elastic theory. The procedure asserts that such a phase boundary is preferred if and only if the strains ε^- and ε^+ on either side of the discontinuity can be smoothly connected by a traveling wave constructed within the augmented theory.

Thus, we are looking for smooth steady wave solutions for the system (1) and (2) which have the form $(\varepsilon,\sigma,v)(X,t)=(\hat\varepsilon,\hat\sigma,\hat v)(\xi)$, where $\xi=X-\dot St$, $\dot S=$ const. and satisfy the boundary conditions

$$\lim_{\xi\to\pm\infty}(\hat\varepsilon,\hat\sigma,\hat v)(\xi)=(\varepsilon^\pm,\sigma^\pm=\sigma_{\rm eq}(\varepsilon^\pm),v^\pm), \tag{34}$$

where ε^+, v^+, ε^-, v^- are given values (see also Suliciu, 1990).

From (1) it follows:

$$\rho\dot S\hat v'(\xi)+\hat\sigma'(\xi)=0,\quad \dot S\hat\varepsilon'(\xi)+\hat v'(\xi)=0, \tag{35}$$

where from by using (34) we get

$$\hat{v}(\xi) = v^+ - \dot{S}(\hat{\varepsilon}(\xi) - \varepsilon^+), \quad \hat{\sigma}(\xi) = \sigma^+ + \varrho\dot{S}^2(\hat{\varepsilon}(\xi) - \varepsilon^+). \tag{36}$$

According to (34) and $(36)_2$ the constant steady wave speed $\dot{S}$ is determined by the states to be connected, through relation

$$\varrho\dot{S}^2 = \frac{\sigma_{\mathrm{eq}}(\varepsilon^+) - \sigma_{\mathrm{eq}}(\varepsilon^-)}{\varepsilon^+ - \varepsilon^-} < E. \tag{37}$$

By using the constitutive equation (2) we get that $\varepsilon = \hat{\varepsilon}(\xi)$ must satisfy

$$\dot{S}(E - \varrho\dot{S}^2)\hat{\varepsilon}'(\xi) = -\frac{E}{\mu}|\hat{\sigma}(\xi) - \sigma_{\mathrm{eq}}(\hat{\varepsilon}(\xi))|^{\lambda-1}(\hat{\sigma}(\xi) - \sigma_{\mathrm{eq}}(\hat{\varepsilon}(\xi))), \quad \lim_{\xi\to\pm\infty}\hat{\varepsilon}(\xi) = \varepsilon^{\pm}. \tag{38}$$

We say that a *phase boundary* is admissible for the elastic system if there exists smooth traveling wave solution $\hat{\varepsilon}(\xi)$, $\hat{\sigma}(\xi)$, $\hat{v}(\xi)$ which connects the limit values $(\varepsilon^-, \sigma^- = \sigma_{\mathrm{eq}}(\varepsilon^-), v^-)$ and $(\varepsilon^+, \sigma^+ = \sigma_{\mathrm{eq}}(\varepsilon^+), v^+)$ where ε^+ and ε^- are in distinct phases. This is called the *viscosity admissibility criterion*. In the following we show that the generalized Maxwell's rate-type approach (2) leads to the same admissibility condition as that obtained by Pego (1987) using the Kelvin–Voigt constitutive equation (10) (case $m = 1$), which is equivalent with the so called *chord criterion* (see also Slemrod, 1983).

Indeed, one easily verifies that a smooth solution of the problem (38) exists if and only if

$$\varrho\dot{S}^2 = \frac{\sigma^+ - \sigma^-}{\varepsilon^+ - \varepsilon^-} \geqslant (\leqslant)\frac{\sigma_{\mathrm{eq}}(\varepsilon) - \sigma^+}{\varepsilon - \varepsilon^+} \quad \text{if } \dot{S} > (<)0, \tag{39}$$

for every value ε between ε^+ and ε^-. That means, for $(\varepsilon^+ - \varepsilon^-)\dot{S} > 0$ (or $(\varepsilon^+ - \varepsilon^-)\dot{S} < 0$) the chord which joins $(\varepsilon^+, \sigma_{\mathrm{eq}}(\varepsilon^+))$ to $(\varepsilon^-, \sigma_{\mathrm{eq}}(\varepsilon^-))$ lies *below (above)* the graph of the function $\sigma_{\mathrm{eq}}(\varepsilon)$ for ε between ε^- and ε^+ (see for instance Fig. 2).

Let us remind that any stationary strain discontinuity satisfies the entropy inequality irrespective of the constitutive assumption. Moreover, since the rate-type constitutive equation (2) has the same equilibria as the elastic equation all discontinuous elastic equilibria can be seen as *trivial* viscous limits. Therefore, a stationary strain discontinuity $\dot{S} = 0$ is admissible for the elastic system without any additional condition.

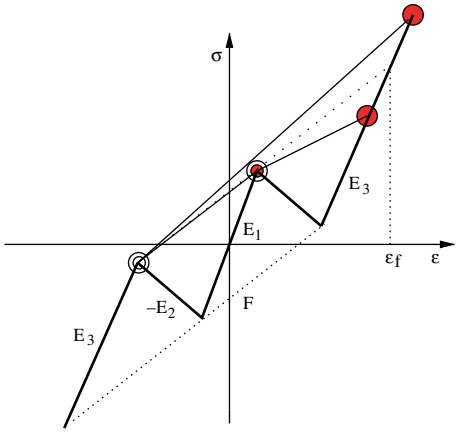

Fig. 2. Subsonic case $E_1 \geqslant E_3 > F$. Admissible waves connecting states $(\varepsilon^+, \sigma_{\mathrm{eq}}(\varepsilon^+))$ (empty circle) and $(\varepsilon^-, \sigma_{\mathrm{eq}}(\varepsilon^-))$ (filled circle) for $\varepsilon^+ < \varepsilon^-$ and $\dot{S} > 0$.

In the following we show that the *total internal dissipation* corresponding to a Maxwellian's type traveling wave is equal with the dissipation induced by an admissible elastic shock wave connecting the states $(\varepsilon^-, \sigma_{\rm eq}(\varepsilon^-))$ and $(\varepsilon^+, \sigma_{\rm eq}(\varepsilon^+))$ for the associated elastic non-monotone equation $\sigma = \sigma_{\rm eq}(\varepsilon)$. That is,

$$D^{\rm tot}_{\rm Mxw} = \int_{-\infty}^{\infty} \frac{E}{\mu}\varrho\frac{\partial\psi}{\partial\sigma}(\hat{\varepsilon}(\xi),\hat{\sigma}(\xi))|\hat{\sigma}(\xi)-\sigma_{\rm eq}(\hat{\varepsilon}(\xi))|^{\lambda-1}(\hat{\sigma}(\xi)-\sigma_{\rm eq}(\hat{\varepsilon}(\xi)))\,{\rm d}\xi$$
$$= \dot{S}\left(\int_{\varepsilon^-}^{\varepsilon^+}\hat{\sigma}(s)\,{\rm d}s - \frac{\sigma_{\rm eq}(\varepsilon^+)+\sigma_{\rm eq}(\varepsilon^-)}{2}(\varepsilon^+-\varepsilon^-)\right) = D_{El}(\varepsilon^+,\varepsilon^-). \tag{40}$$

Proof. Indeed, by using relations (15), (19) and (38) we have

$$D^{\rm tot}_{\rm Mxw} = -\dot{S}(E-\varrho S^2)\int_{-\infty}^{\infty}\frac{\partial\psi}{\partial\sigma}(\hat{\varepsilon}(\xi),\hat{\sigma}(\xi))\hat{\varepsilon}'(\xi)\,{\rm d}\xi$$
$$= -\dot{S}(E-\varrho S^2)\int_{-\infty}^{\infty}\left(\hat{\varepsilon}(\xi)-h^{-1}(\hat{\sigma}(\xi)-E\hat{\varepsilon}(\xi))\right)\hat{\varepsilon}'(\xi)\,{\rm d}\xi. \tag{41}$$

By using relation $(36)_2$ we can write

$$D^{\rm tot}_{\rm Mxw} = -\dot{S}(E-\varrho S^2)\int_{\varepsilon^-}^{\varepsilon^+}\left(\varepsilon - h^{-1}[\sigma + -\varrho\dot{S}^2\varepsilon^+ + (\varrho\dot{S}^2-E)\varepsilon]\right){\rm d}\varepsilon$$
$$= -\frac{\dot{S}(E-\varrho S^2)}{2}((\varepsilon^+)^2-(\varepsilon^-)^2) - \dot{S}\int_{h(\varepsilon^-)}^{h(\varepsilon^+)}h^{-1}(\lambda)\,{\rm d}\lambda = D_{El}(\varepsilon^+,\varepsilon^-), \tag{42}$$

where we have used the identity

$$\int_{h(\varepsilon^-)}^{h(\varepsilon^+)}h^{-1}(\lambda)\,{\rm d}\lambda = \varepsilon^+h(\varepsilon^+) - \varepsilon^-h(\varepsilon^-) - \int_{\varepsilon^-}^{\varepsilon^+}h(s)\,{\rm d}s.$$

Let also note that if we multiply relation (38) by $\sigma_{\rm eq}(\hat{\varepsilon}(\xi)) - \hat{\sigma}(\xi)$ and then integrate it with respect to ξ we get after some simple calculations relation

$$\int_{-\infty}^{\infty}|\sigma_{\rm eq}(\hat{\varepsilon}(\xi))-\hat{\sigma}(\xi)|^{\lambda+1}\,{\rm d}\xi = \mu\frac{E-\varrho\dot{S}^2}{E}D_{El}(\varepsilon^+,\varepsilon^-), \tag{43}$$

which proves that a sharp phase boundary which will arise in the limit of vanishing viscosity $\mu \to 0$ will satisfy the entropy admissibility condition $D_{El}(\varepsilon^+,\varepsilon^-) \geqslant 0$.

The traveling wave solutions for the generalized Kelvin–Voigt's material (10) are obtained from Eq. (38) by making $E \to \infty$. The total dissipation corresponding to this traveling wave can be obtained from (23) and (43) by making $E \to \infty$. We get

$$D^{\rm tot}_{\rm KV} = \int_{-\infty}^{\infty}D_{\rm KV}(\hat{\varepsilon}(\xi),\hat{\sigma}(\xi))\,{\rm d}\xi = \frac{1}{\mu}\int_{-\infty}^{\infty}|\hat{\sigma}(\xi)-\sigma_{\rm eq}(\varepsilon(\xi))|^{\lambda+1}\,{\rm d}\xi = D_{El}(\varepsilon^+,\varepsilon^-). \tag{44}$$

Therefore, for the Kelvin–Voigt's model the total dissipation of a steady wave solution is also the dissipation induced by the corresponding admissible shock wave in the frame of the elastic theory.

Let us note that the magnitude of the total internal dissipation corresponding to a smooth steady wave solution for both rate-type models does not depend on the viscosity parameter μ and on the rate sensitivity parameter λ. The viscosity parameter μ, the rate sensitivity parameter λ and the dynamic Young modulus E will influence only the profile of $\varepsilon = \hat{\varepsilon}(\xi)$, $\xi \in (-\infty,\infty)$, i.e., the smooth transition layer which approximates the sharp interface. This problem will be illustrated in the following (see Fig. 3).

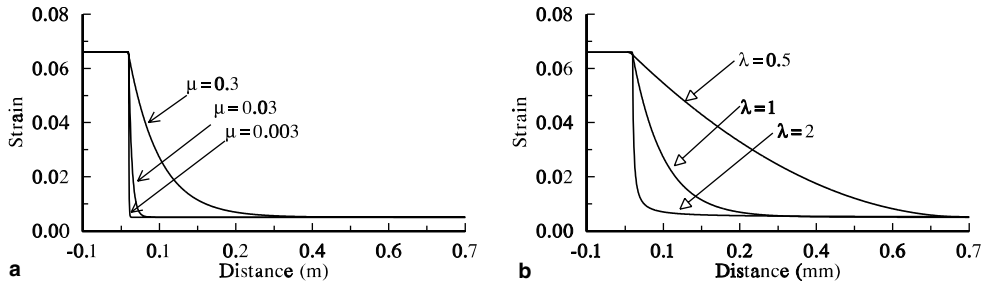

Fig. 3. Traveling wave solution propagating with speed $\dot{S} = 107.4$ m/s connecting states ($\varepsilon_a = 0.005, \sigma_a = 150$ MPa) and ($\varepsilon^- = 0.066, \sigma - = 155$ MPa) for the numerical entries: $E = 31.5$ GPa, $E_1 = E_3 = 30$ GPa, $E_2 = -416.6$ MPa, $\varrho = 7100$ kg/m^3. (a) Influence of the viscosity coefficient μ[MPa s] for $\lambda = 1$. (b) Influence of the rate sensitivity parameter λ for constant $\mu = 0.315$ MPa$^\lambda$ s.

Let us consider the piecewise linear equilibrium curve (4) in the *subsonic case* $E_1 \geqslant E_3 > \frac{\sigma_m+\sigma_a}{\varepsilon_m+\varepsilon_a} \equiv F > 0$. In this case the speed $\dot{S}$ of any admissible phase boundary is always lower than the speed of propagation of the elastic shock waves of either of the homogeneous phases, i.e. $\varrho\dot{S}^2 < E_1$ and $\varrho\dot{S}^2 < E_3$.

Let us consider for instance the case $\dot{S} > 0$ and $\varepsilon^+ < \varepsilon^-$. The possible steady wave solutions traveling to the right depend on the positions of ε^+ and ε^-, and are illustrated in Fig. 2. We analyze in the following only the case of a wave connecting the equilibrium states ($\varepsilon^+ = \varepsilon_a, \sigma^+ = \sigma_a$), corresponding to the maximal stress in $\mathscr{A}$-phase and ($\varepsilon^-, \sigma^- = E_3\varepsilon^- - \sigma_3$) in $\mathscr{M}^+$-phase. In order to satisfy relation (37) and the chord criterion, the following conditions have to be fulfilled $\sigma^- > \sigma_a$ and $\varepsilon^- > \varepsilon_m + \frac{E_2}{E_3}(\varepsilon_m - \varepsilon_a)$. The wave speed is given by $\varrho\dot{S}^2 = E_3 - (E_3 + E_2)(\varepsilon_m - \varepsilon_a)/(\varepsilon^- - \varepsilon_a)$.

By integrating the differential equation (38) we get:

- if $\lambda = 1$ the solution is

$$\hat{\varepsilon}(\xi) = \begin{cases} \varepsilon^- + (\varepsilon_m - \varepsilon^-)\exp\left(\frac{E(E_3-\varrho\dot{S}^2)}{\mu\dot{S}(E-\varrho\dot{S}^2)}(\xi - \xi_m)\right), & \xi \in (-\infty, \xi_m), \\ \varepsilon_a + (\varepsilon_m - \varepsilon_a)\exp\left(\frac{-E(E_2+\varrho\dot{S}^2)}{\mu\dot{S}(E-\varrho\dot{S}^2)}(\xi - \xi_m)\right), & \xi \in (\xi_m, \infty), \end{cases} \tag{45}$$

- if $\lambda \neq 1$ the solution is

$$\hat{\varepsilon}(\xi) = \begin{cases} \varepsilon_a, & \xi \in [\xi^+, \infty), \\ \varepsilon_a + \left[(\varepsilon_m - \varepsilon_a)^{1-\lambda} - \frac{1-\lambda}{\mu}\frac{E(E_2+\varrho\dot{S}^2)^\lambda}{\dot{S}(E-\varrho\dot{S}^2)}(\xi - \xi_m)\right]^{\frac{1}{1-\lambda}}, & \xi \in [\xi_m, \xi^+), \\ \varepsilon^- - \left[(\varepsilon^- - \varepsilon_m)^{1-\lambda} - \frac{1-\lambda}{\mu}\frac{E(E_3-\varrho\dot{S}^2)^\lambda}{\dot{S}(E-\varrho\dot{S}^2)}(\xi_m - \xi)\right]^{\frac{1}{1-\lambda}}, & \xi \in [\xi^-, \xi_m], \\ \varepsilon^-, & \xi \in (-\infty, \xi^-). \end{cases} \tag{46}$$

For $\lambda > 1$, $\xi^+ = \infty$ and $\xi^- = -\infty$, while for $\lambda \in (0, 1)$ we have

$$\begin{aligned} \xi^+ &= \xi_m + \frac{\mu}{1-\lambda}\frac{\dot{S}(E-\varrho\dot{S}^2)}{E(E_2+\varrho\dot{S}^2)^\lambda}(\varepsilon_m - \varepsilon_a)^{1-\lambda}, \\ \xi^- &= \xi_m - \frac{\mu}{1-\lambda}\frac{\dot{S}(E-\varrho\dot{S}^2)}{E(E_3-\varrho\dot{S}^2)^\lambda}(\varepsilon^- - \varepsilon_m)^{1-\lambda}. \end{aligned} \tag{47}$$

In this case,

$$\xi^+ - \xi^- = \frac{\mu}{1-\lambda}\frac{\dot{S}(E-\varrho\dot{S}^2)}{E}\left[\frac{(\varepsilon_m-\varepsilon_a)^{1-\lambda}}{(E_2+\varrho\dot{S}^2)^{\lambda}}+\frac{(\varepsilon^- -\varepsilon_m)^{1-\lambda}}{(E_3-\varrho\dot{S}^2)^{\lambda}}\right]>0 \tag{48}$$

may be called the thickness of the steady wave.

It is obvious now that when the viscosity coefficient $\mu \to 0$ the profile $\varepsilon = \hat{\varepsilon}(\xi)$ of the traveling wave becomes steeper and the transition layer becomes narrow (Fig. 3a). The same effect is obtained when the rate sensitivity λ increases (Fig. 3b). The existence of a finite thickness of a steady wave for $\lambda < 1$ is only apparently an advantage. In Fig. 3b) for $\lambda = 0.5$ the thickness of the traveling wave is $\xi^+ - \xi^- = 0.74$ m, i.e. very large. For $\lambda \geqslant 1$ the thickness of the transition layer is a matter of convention. It is important to mention here that usually the case $\lambda \in (0,1)$ for the generalized Maxwellian rate-type constitutive equation (2), that is the case $m > 1$ for the generalized Kelvin–Voigt constitutive equation (10) is not a physical one for visco-plastic materials.

5. Propagation of disturbances in a pure phase

In this section we investigate the propagation of the waves described by the Maxwellian constitutive equation (2), for $\lambda = 1$, when the material is in a pure phase. We show following Whitham (1959) and Brun and Molinari (1982) that different levels of approximation to the governing equations lead to completely different types of wave motion. In fact, we want to know which set of waves are the most important and will really be observed and to determine the speeds at which the disturbances travel. In order to realize this investigation, we use perturbation methods to obtain simple representations of the solution and a better understanding of physical aspects.

The linear rate-type system of PDEqs governing the wave motion in a pure phase of the material is:

$$\varrho\frac{\partial v}{\partial t}-\frac{\partial \sigma}{\partial X}=0,\quad \frac{\partial \varepsilon}{\partial t}-\frac{\partial v}{\partial X}=0,\quad \frac{\partial \sigma}{\partial t}-E\frac{\partial \varepsilon}{\partial t}=-\frac{E}{\mu}(\sigma-E_0\varepsilon+s), \tag{49}$$

where E_0 represents the elastic modulus of the phase and is equal with $E_1 > 0$, or $-E_2 < 0$, or $E_3 > 0$ and $s = \text{const.}$ is a known constant.

We consider an initial value problem

$$(\varepsilon,\sigma,v)(X,0) = (\varepsilon^*(X),\sigma^*(X),v^*(X)),\quad \text{for } X\in\mathbb{R}, \tag{50}$$

where ε^*, σ^* and v^* are given functions whose class will be specified latter.

The method of multiple scales have since long proved efficient in the solution of dynamical problems (see for instance Jeffrey and Taniuti, 1964; Nayfeh, 1973). The adequate perturbation parameter is built on an arbitrary time scale appearing in a natural way while reducing the equations to a non-dimensional form.

Let us denote by $T > 0$ a characteristic time and by $\Omega > 0$ a characteristic speed. The characteristic time T is an arbitrary quantity and will be called *time scale* while the quantity $\Omega\, T$ is called *space scale*. By performing the following change of independent variables

$$\tilde{t} = \frac{t}{T}\quad \text{and}\quad \widetilde{X} = \frac{X}{\Omega T}, \tag{51}$$

the system (49) becomes

$$\frac{\partial \tilde{v}}{\partial \tilde{t}}-\frac{\partial \tilde{\sigma}}{\partial \widetilde{X}}=0,\quad \frac{\partial \tilde{\varepsilon}}{\partial \tilde{t}}-\frac{\partial \tilde{v}}{\partial \widetilde{X}}=0,\quad \frac{\partial \tilde{\sigma}}{\partial \tilde{t}}-\widetilde{E}\frac{\partial \tilde{\varepsilon}}{\partial \tilde{t}}=-\widetilde{E}\eta(\tilde{\sigma}-\widetilde{E}_0\tilde{\varepsilon}+\tilde{s}), \tag{52}$$

where

$$\tilde{v} = \frac{v}{\Omega}, \quad \tilde{\varepsilon} = \varepsilon, \quad \tilde{\sigma} = \frac{\sigma}{\varrho\Omega^2}, \quad \widetilde{E} = \frac{E}{\varrho\Omega^2}, \quad \widetilde{E}_0 = \frac{E_0}{\varrho\Omega^2}, \quad \tilde{s} = \frac{s}{\varrho\Omega^2} \tag{53}$$

are dimensionless quantities and

$$\eta = (\varrho\Omega^2)\frac{T}{\mu} \tag{54}$$

is a perturbation parameter which is related to the time scale.

5.1. Instantaneous waves—behavior of the waves near the source

We first consider the case of a *small time scale* T, that is a small non-dimensional parameter

$$\eta_1 = (\varrho\Omega^2)\frac{T}{\mu} \ll 1. \tag{55}$$

We look for an approximate solution of the initial problem (49) and (50) of the form:

$$\tilde{u} = \tilde{u}(\tilde{t}, \widetilde{X}, \eta_1) = u_0(t_0, t_1, \ldots, X_0) + \eta_1 u_1(t_0, t_1, \ldots, X_0) + \ldots, \tag{56}$$

where

$$X_0 = \widetilde{X}, \quad t_0 = \tilde{t}, \quad t_1 = \eta_1\tilde{t}, \ldots t_n = (\eta_1)^n\tilde{t}, \quad n \in \mathbb{N} \tag{57}$$

are multiple variables and $\tilde{u}$ stands for $\tilde{\varepsilon}$, $\tilde{\sigma}$ or $\tilde{v}$.

In the following we use the hypothesis that we have next to a "fast time scale" t_0 only the "slow time scale" t_1. Substituting (57) into (52) and taking into account that the partial derivatives with respect to $\tilde{t}$ and $\widetilde{X}$ satisfy relations

$$\frac{\partial\tilde{u}}{\partial\widetilde{X}} = \frac{\partial u_0}{\partial X_0} + \eta_1\frac{\partial u_1}{\partial X_0} \quad \text{and} \quad \frac{\partial\tilde{u}}{\partial\tilde{t}} = \frac{\partial u_0}{\partial t_0} + \eta_1\left(\frac{\partial u_0}{\partial t_1} + \frac{\partial u_1}{\partial t_0}\right), \tag{58}$$

we get after identifying the powers of η_1 the following two systems for the first and second order approximations

$$\frac{\partial v_0}{\partial t_0} - \frac{\partial\sigma_0}{\partial X_0} = 0, \quad \frac{\partial\varepsilon_0}{\partial t_0} - \frac{\partial v_0}{\partial X_0} = 0, \quad \frac{\partial\sigma_0}{\partial t_0} - \widetilde{E}\frac{\partial\varepsilon_0}{\partial t_0} = 0, \tag{59}$$

$$\frac{\partial v_1}{\partial t_0} - \frac{\partial\sigma_1}{\partial X_0} = -\frac{\partial v_0}{\partial t_1}, \quad \frac{\partial\varepsilon_1}{\partial t_0} - \frac{\partial v_1}{\partial X_0} = -\frac{\partial\varepsilon_0}{\partial t_1}, \quad \frac{\partial\sigma_1}{\partial t_0} - \widetilde{E}\frac{\partial\varepsilon_1}{\partial t_0} = \frac{\partial\sigma_0}{\partial t_1} + \widetilde{E}\frac{\partial\varepsilon_0}{\partial t_1} - \widetilde{E}(\sigma_0 - \widetilde{E}_0\varepsilon_0 + \tilde{s}), \tag{60}$$

First order approximation. The general solution of (59) is simply

$$\begin{aligned} v_0(t_0, t_1, X_0) &= f(\gamma_0, t_1) + g(\vartheta_0, t_1), \\ \sigma_0(t_0, t_1, X_0) &= -\sqrt{\widetilde{E}}(f(\gamma_0, t_1) - g(\vartheta_0, t_1)), \\ \varepsilon_0(t_0, t_1, X_0) &= -\frac{1}{\sqrt{\widetilde{E}}}(f(\gamma_0, t_1) - g(\vartheta_0, t_1)) + b(X_0, t_1), \end{aligned} \tag{61}$$

where

$$\gamma_0 = X_0 - \sqrt{\widetilde{E}}t_0 \quad \text{and} \quad \vartheta_0 = X_0 + \sqrt{\widetilde{E}}t_0, \tag{62}$$

and functions $f = f(\gamma_0, t_1), g = g(\vartheta_0, t_1)$ and $b = b(X_0, t_1)$ are supposed to be smooth functions on the slow time variable t_1.

Second order approximation. The second order solution satisfies the following system written in characteristic form by using the characteristic variables γ_0 and ϑ_0 and t_0 as

$$\begin{aligned}
\frac{\partial p_1}{\partial \gamma_0}(\gamma_0,\vartheta_0,t_1) &= \frac{\partial g}{\partial t_1}(\vartheta_0,t_1) + \frac{\widetilde{E}-\widetilde{E}_0}{2}(g(\vartheta_0,t_1)-f(\gamma_0,t_1)) - \frac{\widetilde{E}_0\sqrt{\widetilde{E}}}{2}b\left(\frac{\gamma_0+\vartheta_0}{2},t_1\right) + \frac{\sqrt{\widetilde{E}}}{2}\tilde{s},\\
\frac{\partial q_1}{\partial \vartheta_0}(\gamma_0,\vartheta_0,t_1) &= \frac{\partial f}{\partial t_1}(\gamma_0,t_1) - \frac{\widetilde{E}-\widetilde{E}_0}{2}(g(\vartheta_0,t_1)-f(\gamma_0,t_1)) + \frac{\widetilde{E}_0\sqrt{\widetilde{E}}}{2}b\left(\frac{\gamma_0+\vartheta_0}{2},t_1\right) - \frac{\sqrt{\widetilde{E}}}{2}\tilde{s},\\
\frac{\partial r_1}{\partial t_0}(t_0,t_1,X_0) &= \widetilde{E}\left(\frac{\partial b}{\partial t_1}(X_0,t_1) + \widetilde{E}_0 b(X_0,t_1) - \tilde{s}\right) - \sqrt{\widetilde{E}}(\widetilde{E}-\widetilde{E}_0)(g(\vartheta_0,t_1)-f(\gamma_0,t_1)),
\end{aligned} \tag{63}$$

where

$$p_1 = \sigma_1 + \sqrt{\widetilde{E}}v_1, \quad q_1 = \sigma_1 - \sqrt{\widetilde{E}}v_1, \quad r_1 = \sigma_1 - \widetilde{E}\varepsilon_1. \tag{64}$$

The terms on the right-hand side of (63) which do not depend on the corresponding integration variables must be eliminated since they would lead to unbounded terms in p_1, q_1 and r_1, respectively, that is to secular terms in the asymptotic development (56). Therefore the following conditions have to be satisfied

$$\begin{aligned}
&\frac{\partial g}{\partial t_1}(\vartheta_0,t_1) + \frac{\widetilde{E}-\widetilde{E}_0}{2}g(\vartheta_0,t_1) + \frac{\sqrt{\widetilde{E}}}{2}\tilde{s} = 0,\\
&\frac{\partial f}{\partial t_1}(\gamma_0,t_1) + \frac{\widetilde{E}-\widetilde{E}_0}{2}f(\gamma_0,t_1) - \frac{\sqrt{\widetilde{E}}}{2}\tilde{s} = 0,\\
&\frac{\partial b}{\partial t_1}(X_0,t_1) + \widetilde{E}_0 b(X_0,t_1) - \tilde{s} = 0.
\end{aligned} \tag{65}$$

The general solutions of the above equations are

$$\begin{aligned}
g(\vartheta_0,t_1) &= G(\vartheta_0)\exp\left(-\frac{\widetilde{E}-\widetilde{E}_0}{2}t_1\right) - \frac{\sqrt{\widetilde{E}}}{\widetilde{E}-\widetilde{E}_0}\tilde{s},\\
f(\gamma_0,t_1) &= F(\gamma_0)\exp\left(-\frac{\widetilde{E}-\widetilde{E}_0}{2}t_1\right) + \frac{\sqrt{\widetilde{E}}}{\widetilde{E}-\widetilde{E}_0}\tilde{s},\\
b(X_0,t_1) &= B(X_0)\exp(-\widetilde{E}_0 t_1) + \frac{1}{\widetilde{E}_0}\tilde{s},
\end{aligned} \tag{66}$$

respectively, where functions G, F and B have to be determined from the initial conditions (50).

By returning to the physical variables and by using the initial data (50) we can write the solution near the source of a perturbation as

$$\begin{aligned}
v(t,X) &\simeq \left(\frac{v^*(\gamma)+v^*(\vartheta)}{2} + \frac{\sigma^*(\gamma)-\sigma^*(\vartheta)}{2\sqrt{\varrho E}}\right)\exp\left(-\frac{E-E_0}{2\mu}t\right),\\
\sigma(t,X) &\simeq \left(\frac{\sigma^*(\gamma)+\sigma^*(\vartheta)}{2} - \frac{v^*(\gamma)-v^*(\vartheta)}{\sqrt{\varrho E}} + \frac{2E}{E-E_0}s\right)\exp\left(-\frac{E-E_0}{2\mu}t\right) - \frac{2E}{E-E_0}s,\\
\varepsilon(t,X) &\simeq \frac{1}{E}\sigma(t,X) + \left(\varepsilon^*(X) - \frac{1}{E}\sigma^*(X) - \frac{1}{E_0}s\right)\exp\left(-\frac{E_0}{\mu}t\right) + \frac{1}{E_0}s,
\end{aligned} \tag{67}$$

where $\gamma = X - \sqrt{\frac{E}{\varrho}}t$, and $\vartheta = X + \sqrt{\frac{E}{\varrho}}t$.

Since the physical variables X, t and the dimensionless variables X_0, t_0, t_1 are related through relations $X-\sqrt{E/\varrho}t=\Omega T(X_0-\sqrt{\widetilde{E}}t_0)$, $X+\sqrt{E/\varrho}t=\Omega T(X_0+\sqrt{\widetilde{E}}t_0)$, and $t=\frac{\mu}{\varrho\Omega^2}t_1$ and since the time scale T has been supposed small it follows that relations (67) are a good approximation of the solution of the initial problem (50) for the system (49) in the neighborhood of the fronts propagating with the velocities $\pm\sqrt{\frac{E}{\varrho}}$. Moreover, since the slow variable t_1 is small it follows that this representation is valid for a small time interval $t\leqslant t_1$. These solutions are called *instantaneous waves* and describe the behavior of the waves near the source of a perturbation.

Consequently, from $(67)_{1,2}$ it follows that the instantaneous waves are exponentially damped near the wave-fronts moving with the speeds $\pm\sqrt{\frac{E}{\varrho}}$ and become negligible when $t\gg\frac{2\mu}{E-E_0}$. Another important consequence is revealed by relation $(67)_3$ which explains how an inhomogeneity of the initial strain or stress field (such that $\sigma^*(X)\neq E\varepsilon^*(X)-\frac{E}{E_0}s$) is *exponentially damped* and becomes negligible when the material lies in one of the stable phases $\mathscr{A}$ or $\mathscr{M}^{\pm}$, that is for $E_0>0$, or it is *exponentially blown up* when the material enters in the unstable phases $\mathscr{I}^{\pm}$, that is for $E_0<0$.

One of the benefits of our analysis is that it shows that the rate-type model can be seen as a kinetic law since it possesses its own kinetics due to the dissipative viscous mechanism incorporated, without the need of a separate nucleation criterion. Indeed, formula $(67)_3$ clarifies how the nucleation appears when particles of the bars enter in the unstable intervals and how the phases can growth leading to the emergence of stationary phase boundaries. Let us note that the rate at which the materials transforms is characterized by the *growth factor* E_2/μ in the *unstable phase* of the material $I^+\equiv(\varepsilon_a,\varepsilon_m)$ and by the *damping factor* $-E_3/\mu$ in the stable phase of the material $\mathscr{M}^+\equiv[\varepsilon_m,\infty))$, for example. These stability/instability parameters are the same as in relations (11) illustrated in Fig. 1a.

Let us also note the agreement between solution (67) and relations describing the variation of a jump of strain along the strong discontinuities of the Maxwellian hyperbolic semilinear system. Indeed, the jump of strain $[\varepsilon]$ *along a discontinuity propagating* with speeds $\dot{S}=\pm\sqrt{E/\varrho}$ is always exponentially damped according to relation $[\varepsilon](t)=[\varepsilon](0)\exp(-\frac{E-E_0}{2\mu}t)$, while *along a stationary discontinuity* $\dot{S}=0$ it is exponentially *damped or amplified*, depending on the sign of E_0, according to relation $[\varepsilon](t)=[\varepsilon](0)\exp(-\frac{E_0}{\mu}t)$, where E_0 is equal with the slope of the equilibrium curve, i.e., $E_1>0$, $-E_2<0$, or $E_3>0$ (see Făciu, 1996).

It is clear that when the material is in the stable phases $\mathscr{A}$, or $\mathscr{M}^{\pm}$ (i.e. when $E_0>0$) after a time interval the main part of a disturbance is away from the instantaneous wave fronts. To locate it, we investigate the behavior of the solution of the initial-boundary value problem (49), (50) for large t.

5.2. Delayed waves—behavior of the waves far from the source

We consider the case of a *large time scale* T, that is a small non-dimensional parameter

$$\eta_2=(\varrho\Omega^2)^{-1}\frac{\mu}{T}\ll 1. \tag{68}$$

By using the change of independent variables (51) the system (49) becomes

$$\frac{\partial\tilde{v}}{\partial\tilde{t}}-\frac{\partial\tilde{\sigma}}{\partial\widetilde{X}}=0,\quad \frac{\partial\tilde{\varepsilon}}{\partial\tilde{t}}-\frac{\partial\tilde{v}}{\partial\widetilde{X}}=0,\quad \eta_2\left(\frac{\partial\tilde{\sigma}}{\partial\tilde{t}}-\widetilde{E}\frac{\partial\tilde{\varepsilon}}{\partial\tilde{t}}\right)=-\widetilde{E}(\tilde{\sigma}-\widetilde{E}_0\tilde{\varepsilon}+\tilde{s}), \tag{69}$$

Our goal is to investigate the long time behavior of the solution of the problem (49) + (50). In order to take into account the behavior of the solution for earlier times, too, that is the influence of the initial data, we use the following multiple variables

$$X_0=\widetilde{X},\quad t_0=\frac{\tilde{t}}{\eta_2},\quad t_1=\tilde{t},\quad t_2=\tilde{t}\eta_2,\ \ldots\quad t_n=\tilde{t}(\eta_2)^{n-1},\quad n\in\mathbb{N},\quad n>3. \tag{70}$$

We now look for an approximate solution of the form

$$\tilde{u} = \tilde{u}(\tilde{t}, \widetilde{X}, \eta_2) = u_0(t_0, t_1, t_2, \ldots, X_0) + \eta_2 u_1(t_0, t_1, t_2, \ldots, X_0) + \cdots, \tag{71}$$

where $\tilde{u}$ stands for $\tilde{\varepsilon}$, $\tilde{\sigma}$ and $\tilde{v}$.

In the following we only consider the case of three time scales t_0, t_1 and t_2. The first one is a fast time scale and gives account on a boundary layer solution necessary to adjust the initial data, the second one is an intermediate time variable, while the third one is a slow variable which describes the long time behavior of the solution. After substituting (71) into (69) and taking into account that the partial derivatives of $\tilde{u}$ with respect to $\tilde{t}$ and $\widetilde{X}$ satisfy relations

$$\frac{\partial \tilde{u}}{\partial \widetilde{X}} = \frac{\partial u_0}{\partial X_0} + \eta_2 \frac{\partial u_1}{\partial X_0} \quad \text{and} \quad \frac{\partial \tilde{u}}{\partial \tilde{t}} = \frac{1}{\eta_2}\frac{\partial u_0}{\partial t_0} + \left(\frac{\partial u_0}{\partial t_1} + \frac{\partial u_1}{\partial t_0}\right) + \eta_2\left(\frac{\partial u_0}{\partial t_2} + \frac{\partial u_1}{\partial t_1}\right), \tag{72}$$

we get after identifying the powers of η_2 the following systems for the approximations of order $\mathcal{O}(1/\eta_2)$, $\mathcal{O}(1)$ and $\mathcal{O}(\eta_2)$, respectively

$$\frac{\partial v_0}{\partial t_0} = 0, \quad \frac{\partial \varepsilon_0}{\partial t_0} = 0, \quad \frac{\partial \sigma_0}{\partial t_0} - \widetilde{E}\frac{\partial \varepsilon_0}{\partial t_0} = -\widetilde{E}(\sigma_0 - \widetilde{E}_0\varepsilon_0 + \tilde{s}), \tag{73}$$

$$\frac{\partial v_1}{\partial t_0} = \frac{\partial \sigma_0}{\partial X_0} - \frac{\partial v_0}{\partial t_1}, \quad \frac{\partial \varepsilon_1}{\partial t_0} = \frac{\partial v_0}{\partial X_0} - \frac{\partial \varepsilon_0}{\partial t_1}, \quad \frac{\partial \sigma_1}{\partial t_0} - \widetilde{E}\frac{\partial \varepsilon_1}{\partial t_0} + \widetilde{E}(\sigma_1 - \widetilde{E}_0\varepsilon_1) = -\frac{\partial \sigma_0}{\partial t_1} + \widetilde{E}\frac{\partial \varepsilon_0}{\partial t_1}, \tag{74}$$

$$\frac{\partial v_1}{\partial t_1} - \frac{\partial \sigma_1}{\partial X_0} = -\frac{\partial v_0}{\partial t_2}, \quad \frac{\partial \varepsilon_1}{\partial t_1} - \frac{\partial v_1}{\partial X_0} = -\frac{\partial \varepsilon_0}{\partial t_2}, \quad \frac{\partial \sigma_1}{\partial t_1} - \widetilde{E}\frac{\partial \varepsilon_1}{\partial t_1} = \frac{\partial \sigma_0}{\partial t_2} - \widetilde{E}\frac{\partial \varepsilon_0}{\partial t_2}. \tag{75}$$

The general solution of the system (73) is

$$\begin{aligned} &v_0 = v_0(t_1, t_2, X_0), \\ &\varepsilon_0 = \varepsilon_0(t_1, t_2, X_0), \\ &\sigma_0 = \sigma_0(t_0, t_1, t_2, X_0) = C_0(t_1, t_2, X_0)\exp(-\widetilde{E}t_0) + \widetilde{E}_0\varepsilon_0(t_1, t_2, X_0) - \tilde{s}, \end{aligned} \tag{76}$$

where $C_0 = C_0(t_1, t_2, X_0)$ is an arbitrary smooth function. It describes a boundary layer solution.

The system (74) becomes

$$\begin{aligned} &\frac{\partial v_1}{\partial t_0} = -\frac{\partial v_0}{\partial t_1} + \widetilde{E}_0\frac{\partial \varepsilon_0}{\partial X_0} + \frac{\partial C_0}{\partial X_0}\exp(-\widetilde{E}t_0), \\ &\frac{\partial \varepsilon_1}{\partial t_0} = \frac{\partial v_0}{\partial X_0} - \frac{\partial \varepsilon_0}{\partial t_1}, \\ &\frac{\partial(\sigma_1 \exp(\widetilde{E}t_0))}{\partial t_0} = \exp(\widetilde{E}t_0)\left(\widetilde{E}\frac{\partial v_0}{\partial X_0} - \widetilde{E}_0\frac{\partial \varepsilon_0}{\partial t_1} + \widetilde{E}\widetilde{E}_0\varepsilon_1\right) - \frac{\partial C_0}{\partial t_1}. \end{aligned} \tag{77}$$

The terms independent on t_0 on the right hand side of the system (77) must be eliminated since they would lead to unbounded terms in v_1, ε_1 and σ_1. Thus, the following conditions have to be fulfilled

$$\frac{\partial v_0}{\partial t_1} - \widetilde{E}_0\frac{\partial \varepsilon_0}{\partial X_0} = 0, \quad \frac{\partial v_0}{\partial X_0} - \frac{\partial \varepsilon_0}{\partial t_1} = 0, \quad \frac{\partial C_0}{\partial t_1} = 0. \tag{78}$$

If $E_0 > 0$ then the system $(78)_{1+2}$ is hyperbolic and its general solution leads to

$$\begin{aligned} &v_0 = v_0(t_1, t_2, X_0) = f(\gamma_0, t_2) + g(\vartheta_0, t_2), \\ &\varepsilon_0 = \varepsilon_0(t_1, t_2, X_0) = -\frac{1}{\sqrt{\widetilde{E}_0}}(f(\gamma_0, t_2) - g(\vartheta_0, t_2)), \\ &\sigma_0 = \sigma_0(t_0, t_1, t_2, X_0) = C_0(t_2, X_0)\exp(-\widetilde{E}t_0) + \widetilde{E}_0\varepsilon_0(t_1, t_2, X_0) - \tilde{s}, \end{aligned} \tag{79}$$

where

$$\gamma_0 = X_0 - \sqrt{\widetilde{E}_0}t_1 \quad \text{and} \quad \vartheta_0 = X_0 + \sqrt{\widetilde{E}_0}t_1, \tag{80}$$

and functions $f = f(\gamma_0, t_2)$ and $g = g(\vartheta_0, t_2)$ are arbitrary smooth functions on the slow time variable t_2. Let us note that relations (79) describe the propagation of a disturbance with the speed $\sqrt{E_0/\varrho}$ which are lower than the speed of the instantaneous wave $\sqrt{E/\varrho}$ where from their denomination of *delayed waves*.

If $E_0 < 0$ then the system $(78)_{1+2}$ is elliptic and any initial value problem is ill-posed for it. Therefore in the unstable phases there will be no delayed wave solutions.

By replacing now relations (79) in the system (77) and integrating it, we get the following form of the second approximation

$$\begin{aligned}
&v_1 = v_1(t_0, t_1, t_2, X_0) = -\frac{1}{\widetilde{E}_0}\frac{\partial C_0}{\partial X_0}(t_2, X_0)\exp(-\widetilde{E}t_0) + w_1(t_1, t_2, X_0),\\
&\varepsilon_1 = \varepsilon_1(t_1, t_2, X_0),\\
&\sigma_1 = \sigma_1(t_0, t_1, t_2, X_0,) = C_1(t_1, t_2, X_0)\exp(-\widetilde{E}t_0) + \widetilde{E}_0\varepsilon_1(t_1, t_2, X_0) + \frac{\widetilde{E} - \widetilde{E}_0}{\widetilde{E}}\left(\frac{\partial f}{\partial \gamma_0} + \frac{\partial g}{\partial \vartheta_0}\right).
\end{aligned} \tag{81}$$

where $w_1 = w_1(t_1, t_2, X_0)$ and $C_1 = C_1(t_1, t_2, X_0)$ are two arbitrary functions on their variables.

By using expressions (79) and (81) in the system (75) of the order $\mathcal{O}(\eta_2)$ we get the following system for the unknowns $w_1 = w_1(t_1, t_2, X_0)$, $C_1 = C_1(t_1, t_2, X_0)$ and $\varepsilon_1 = \varepsilon_1(t_1, t_2, X_0)$, which can be written in the characteristic form

$$\frac{\partial p_1}{\partial \gamma_0} = -2\frac{\partial g}{\partial t_2}(\vartheta_0, t_2) + \frac{\widetilde{E} - \widetilde{E}_0}{\widetilde{E}}\frac{\partial^2 g}{\partial \vartheta_0^2}(\vartheta_0, t_2) + \frac{\widetilde{E} - \widetilde{E}_0}{\widetilde{E}}\frac{\partial^2 f}{\partial \gamma_0^2} + \exp(-\widetilde{E}t_0)\left(\frac{\partial C_1}{\partial X_0} - \frac{1}{\sqrt{\widetilde{E}_0}}\frac{\partial^2 C_0}{\partial X_0^2}\right), \tag{82}$$

$$\frac{\partial q_1}{\partial \vartheta_0} = -2\frac{\partial f}{\partial t_2}(\gamma_0, t_2) + \frac{\widetilde{E} - \widetilde{E}_0}{\widetilde{E}}\frac{\partial^2 f}{\partial \gamma_0^2}(\gamma_0, t_2) + \frac{\widetilde{E} - \widetilde{E}_0}{\widetilde{E}}\frac{\partial^2 g}{\partial \vartheta_0^2} + \exp(-\widetilde{E}t_0)\left(\frac{\partial C_1}{\partial X_0} + \frac{1}{\sqrt{\widetilde{E}_0}}\frac{\partial^2 C_0}{\partial X_0^2}\right), \tag{83}$$

$$\frac{\partial r_1}{\partial t_1} = -\exp(-\widetilde{E}t_0)\frac{\partial C_0}{\partial t_2}(t_2, X_0) - \frac{\widetilde{E} - \widetilde{E}_0}{\sqrt{\widetilde{E}_0}}\left(\frac{\partial f}{\partial t_2} - \frac{\partial g}{\partial t_2}\right) + \frac{\sqrt{\widetilde{E}_0}(\widetilde{E} - \widetilde{E}_0)}{\widetilde{E}}\left(\frac{\partial^2 f}{\partial \gamma_0} - \frac{\partial^2 g}{\partial \vartheta_0}\right), \tag{84}$$

where

$$\begin{aligned}
&p_1 = p_1(\gamma_0, \vartheta_0, t_2) = -2\sqrt{\widetilde{E}_0}\left(w_1 + \sqrt{\widetilde{E}_0}\varepsilon_1\right), \quad q_1 = q_1(\gamma_0, \vartheta_0, t_2) = 2\sqrt{\widetilde{E}_0}\left(w_1 - \sqrt{\widetilde{E}_0}\varepsilon_1\right),\\
&r_1 = r_1(t_0, t_1, t_2, X_0) = \exp(-\widetilde{E}t_0)C_1(t_1, t_2, X_0) - (\widetilde{E} - \widetilde{E}_0)\varepsilon_1(t_1, t_2, X_0).
\end{aligned}$$

In order to avoid again secular terms in the asymptotic expansion (71) the terms independent on γ_0 in (82), independent on ϑ_0 in (83) and independent on t_1 in (84) must be eliminated since they would lead to unbounded terms in p_1, q_1 and r_1, respectively, that is in v_1, ε_1 and σ_1. Thus, the following conditions have to be verified

$$\frac{\partial g}{\partial t_2}(\vartheta_0, t_2) = \frac{\widetilde{E} - \widetilde{E}_0}{2\widetilde{E}}\frac{\partial^2 g}{\partial \vartheta_0^2}(\vartheta_0, t_2), \quad \frac{\partial f}{\partial t_2}(\gamma_0, t_2) = \frac{\widetilde{E} - \widetilde{E}_0}{2\widetilde{E}}\frac{\partial^2 f}{\partial \gamma_0^2}(\gamma_0, t_2), \quad \frac{\partial C_0}{\partial t_2}(t_2, X_0) = 0. \tag{85}$$

The general solutions of the diffusion type Eqs. $(85)_{1,2}$ are, respectively,

$$\begin{aligned}
&g(\vartheta_0, t_2) = \frac{1}{2\sqrt{\pi \tilde{a} t_2}}\int_{-\infty}^{\infty} g(s, 0)\exp\left(-\frac{(s - \vartheta_0)^2}{4\tilde{a}t_2}\right)\mathrm{d}s,\\
&f(\gamma_0, t_2) = \frac{1}{2\sqrt{\pi \tilde{a} t_2}}\int_{-\infty}^{\infty} f(s, 0)\exp\left(-\frac{(s - \gamma_0)^2}{4\tilde{a}t_2}\right)\mathrm{d}s,
\end{aligned} \tag{86}$$

where

$$\tilde{a} = \frac{\widetilde{E} - \widetilde{E}_0}{2\widetilde{E}} \tag{87}$$

is a diffusion coefficient and functions $f(s,0)$ and $g(s,0)$ have to be determined from the initial conditions (50).

By returning to the physical variables we get the following representation of the solution

$$\begin{aligned}
v(t,X) &= \frac{1}{2\sqrt{\pi a t}} \int_{-\infty}^{\infty} \left(G(s) \exp\left(-\frac{(s - X - \sqrt{E_0/\varrho}t)^2}{4at} \right) + F(s) \exp\left(-\frac{(s - X + \sqrt{E_0/\varrho}t)^2}{4at} \right) \right) \mathrm{d}s, \\
\varepsilon(t,X) &= \frac{\sqrt{\varrho/E_0}}{2\sqrt{\pi a t}} \int_{-\infty}^{\infty} \left(G(s) \exp\left(-\frac{(s - X - \sqrt{E_0/\varrho}t)^2}{4at} \right) - F(s) \exp\left(-\frac{(s - X + \sqrt{E_0/\varrho}t)^2}{4at} \right) \right) \mathrm{d}s, \\
\sigma(t,X) &= C(X) \exp\left(-\frac{E}{\mu} t \right) + E_0 \varepsilon(t,X) - s,
\end{aligned} \tag{88}$$

where

$$a = \frac{E - E_0}{2E} \frac{\mu}{\varrho}, \tag{89}$$

and functions $F = F(X)$, $G = G(X)$ and $C = C(X)$ are determined from the initial conditions (50) through relations

$$\begin{aligned}
&G(X) = \frac{1}{2}\left(v^*(X) + \sqrt{\frac{E_0}{\varrho}} \varepsilon^*(X) \right), \quad F(X) = \frac{1}{2}\left(v^*(X) - \sqrt{\frac{E_0}{\varrho}} \varepsilon^*(X) \right), \\
&C(X) = \sigma^*(X) - E_0 \varepsilon^*(X) + s.
\end{aligned} \tag{90}$$

Let us note that the first term in $(88)_3$ describes a boundary layer solution which becomes negligible when $t \gg \frac{\mu}{E}$. Hence the thickness of the boundary layer is $\mathcal{O}(\frac{\mu}{E})$.

On the other hand, the above relations show that the disturbances propagate *far from their source* at the speeds $\pm\sqrt{E_0/\varrho}$, spreads out like $\sqrt{at}$, while their amplitude decreases like $1/\sqrt{at}$ which is typical for a diffusion process. The overall nature of the propagation of disturbances for the rate-type model (2) is shown schematically in an x–t diagram in Fig. 4. As usual, the rate-type terms in the constitutive relation (49) are responsible about the diffusion of these waves. This analysis shows that the effect of the dissipative nature of the problem is to transform the instantaneous waves propagating with speeds $\sqrt{E/\varrho}$ into pseudo-waves (called here delayed waves) propagating with slower speeds $\sqrt{E_0/\varrho}$.

Let us analyze some consequences of the relations between the material parameters intervening in the model. The larger is the departure between the dynamic Young modulus E and the elastic modulus E_0 the larger is the diffusivity coefficient a and the larger is the damping factor $(E-E_0)/2\mu$ of the instantaneous waves (67). The *maximal value of the diffusivity coefficient* $a \leqslant \mu/2\varrho$ is attained for the Kelvin–Voigt's model, that is when $E \to \infty$. In this case there are no more instantaneous waves.

On the other side, the diffusion coefficient a is direct proportional with μ, but the damping factor of the instantaneous waves is inverse proportional with μ. That means a low μ transforms rapidly an instantaneous waves in delayed waves with a low diffusivity while for a large μ the diffusivity process is enhanced while the attenuation of the instantaneous waves is delayed.

The behavior of propagating fronts in a pure phase induced by the impact of two bars is illustrated in Fig. 5b. One can see that if μ is low the attenuation of the instantaneous waves appears earlier and

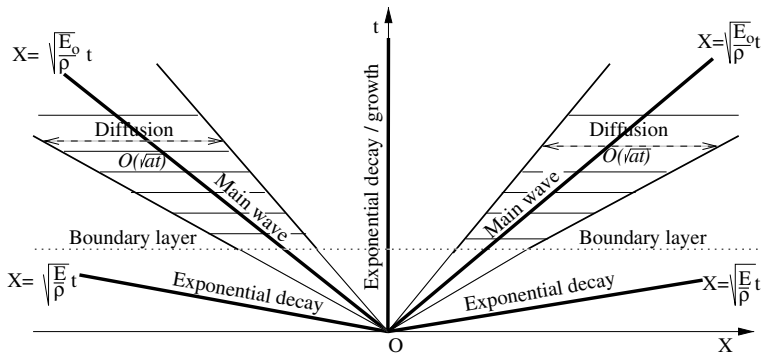

Fig. 4. Representation of the propagating fronts in a single phase for the rate-type material.

the diffusion of the delayed waves appears latter (Fig. 5c) and vice versa (Fig. 5a). Indeed, in Fig. 5a the compressive loading wave arrives at the free end of the target bar as an instantaneous wave at time $t = \frac{l}{C}$, while in Fig. 5c it arrives as a delayed wave at time $t = \frac{l}{C_1}$. The situation in between, when the instantaneous wave transforms in a delayed wave is illustrated by Fig. 5b.

A main benefit of the above analysis is that it explicitly clarifies the role of the material parameters in preventing unwanted diffusivity aspects which can be induced by the rate-type approach. Indeed, since the occurrence of diffusion is not envisaged in phase transition phenomena in shape memory bars, according to relation (89) a closer value of the dynamic Young modulus E to the elastic moduli of the stable phases E_1 and E_3 coupled with a low value of the viscosity coefficient μ will avoid the appearance of diffusive solution in the stable phases of the material. It is useful to note here the advantage of using the Maxwellian rate-type approach instead of the Kelvin–Voigt's approach. While for the Kelvin–Voigt's model the diffusivity can be completely removed only for a null viscosity μ which from kinetic point of view is not

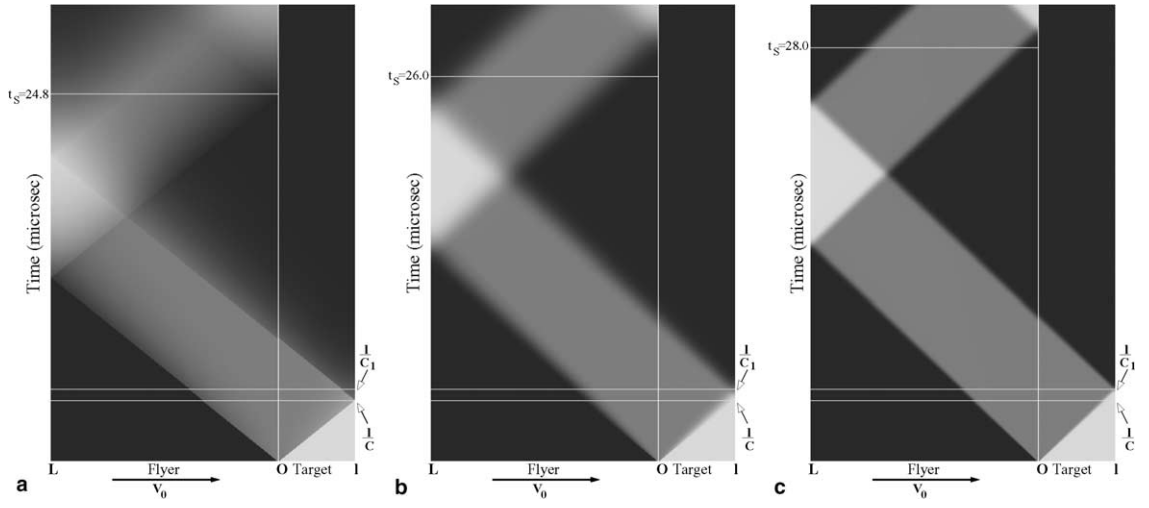

Fig. 5. Velocity distribution in a "viscoelastic" impact of two bars. Influence of the diffusion coefficient $a = (E - E_1)\mu/2\varrho E$ and of the damping factor $(E - E_1)/2\mu$ on the propagating fronts for the numerical entries: $E = 41.5$ GPa, $E_1 = 30$ GPa, $\varrho = 7100$ kg/m^3; (a) $a = 0.8$ m^2/s($\mu = 4.1 \times 10^{-2}$ MPa s) (b) $a = 0.08$ m^2/s($\mu = 4.1 \times 10^{-3}$ MPa s) (c) $a = 0.008$ m^2/s($\mu = 4.1 \times 10^{-4}$ MPa s) where $C = \sqrt{E/\varrho}$ and $C_1 = \sqrt{E/\varrho}$.

suitable since it implies infinite damping factor $-E_3/\mu$ and infinite growth factor E_2/μ in (11), for the Maxwell's type model the diffusivity can be zero without zero viscosity when $E = E_0$. In this case instantaneous and delayed waves coincide.

6. Longitudinal impact of two bars—numerical approach

In the following we investigate the longitudinal impact of two phase transforming bars described by the Maxwellian rate-type model (2) when $\lambda = 1$. For the material parameters appearing in the equilibrium curve (4) we use the following values, appropriate for a NiTi shape memory alloy:

$$E = 95\ \text{GPa}, \quad E_1 = E_3 = 90\ \text{GPa}, \quad E_2 = 3.33\ \text{GPa}, \quad \varrho = 6500\ \text{kg/m}^3,$$
$$\varepsilon_a = 0.005, \quad \sigma_a = 450\ \text{MPa}, \quad \varepsilon_m = 0.065, \quad \sigma_m = 250\ \text{MPa}.$$

For the Newtonian viscosity coefficient μ, we consider values ranging from 9.5×10^{-3} MPa s to 9.5×10^{-4} MPa s which correspond to a Maxwellian viscosity coefficient $k = E/\mu$ ranging from 10^7/s to 10^8/s.

We consider at the initial moment a bar called "target" impacted at the left end by another bar called "flyer" which is moving with a known velocity V_0. After impact the two bars remain in contact and move together until a time t_S called *time of separation*. The time t_S has to be determined when constructing the solution, as the first time when $\sigma(0-, t)$ or $\sigma(0+, t)$ becomes positive, i.e. when the first tensile wave arrives at the contact point $X = 0$. Left end of the flyer and right end of the target are characterized by free stress end conditions. After separation we have also to consider at $X = 0$ free stress end conditions. Such kind of experiments have been frequently used in dynamic plasticity (see, Bell, 1968 and Cristescu and Suliciu, 1982, Chapter IV).

We denote by L the length of the flyer and by l the length of the target and we suppose $L > l$ in order to delay the interaction between the waves reflected at the left end of the flyer with the phase boundaries induced near the impact face. We simulate longitudinal bar impact experiments for a variety of impact conditions for the case $L = 30$ mm and $l = 10$ mm.

In order to determine numerically the evolution in time of the stress, strain and particle velocity in both bars we use a second order accurate method of characteristics with an energetic estimates on the time integration step obtained by Mihăilescu-Suliciu and Suliciu (1992).

Experiments with longitudinal impact of phase transforming bars are an effective mean to investigate the propagation of phase boundaries. Indeed, although a phase boundary propagates, in general, at speeds substantially slower than sound speeds, and therefore never reaches the monitoring surface, its speed can be determined indirectly from the measured particle velocity of this surface. Thus, velocity–time profiles obtained at the free-end of the target bar provide information about the forward and reverse transformation kinetics.

Therefore, we focus here on those numerical results which can be compared with experimental data. These are: the time of separation, which can be accurately determined by optical methods, the velocity at the free-end of the target bar, which can be measured by VISAR interferometer systems and the stress at the impact face, which can be measured by piezoelectric wafers.

Another goal of this numerical investigation is to analyze the difference and the resemblance between the solution of the Maxwellian rate-type model and the solution of the elastic model for the same impact problems.

We have shown in Part I (Făciu and Molinari, 2005) that for the elastic model we have the following results. If the impact velocity V_0 is lower than $V_{ph} = 2\sigma_a/\sqrt{\varrho E_1} = 37.2$ m/s then the contact between the two bars is elastic. Fig. 6a illustrates that this result is described by the Maxwellian rate-type model. Indeed,

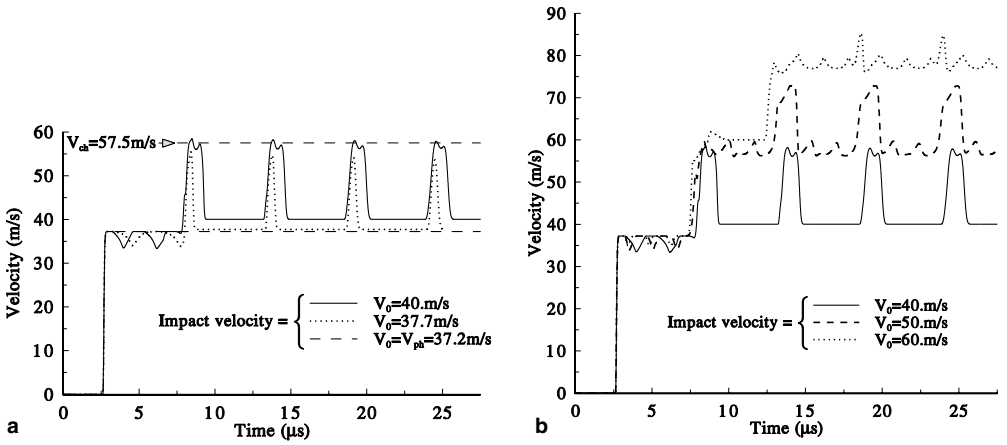

Fig. 6. Influence of the impact velocity on target free-end particle velocity $v(l,t)$ for $\mu = 9.5 \times 10^{-4}$ MPa s ($k = E/\mu = 10^8$/s).

for $V_0 = 37.2$ m/s the free-end particle velocity of the target starts a step-like increase around the time $t = 2.65\ \mu s \in (l/C_1 = 2.61\ \mu s,\ l/C = 2.68\ \mu s)$, $C_1 = \sqrt{E_1/\varrho}$, $C = \sqrt{E/\varrho}$, upon the arrival of a loading wave at the rear end of the target. When the above critical value of the impact velocity is overcome, for example, when $V_0 = 37.7$ m/s or $V_0 = 40$ m/s, then a phase transformation is induced. The presence of a propagating phase boundary near the impact face produces a new increase of the particle velocity at the target free-end. This increase corresponds to the arrival time of a new loading wave reflected by the phase boundary generated by impact. Because the flyer and the target have the same acoustic impedance, no increase in particle velocity is expected at this time if no transformation occurs. This peak of the particle velocity disappears after a few μs. The decay of the particle velocity is in fact the manifestation at the target free-end of the disappearance of the transformed zone in both bars. Indeed, the time of this step-like decay corresponds to the arrival time at $X = l$ of a tensile wave initiated by the beginning of the reverse transformation and is for moderate impact velocity a bit larger than $t_S + l/C_1$ (see for instance Fig. 7a and Fig. 8). After this time moment the velocity peak reproduces at regular time intervals which corresponds to a round trip of an elastic wave in the flyer. The slow decay of the amplitude of this peak for the rate-type model will be analyzed later.

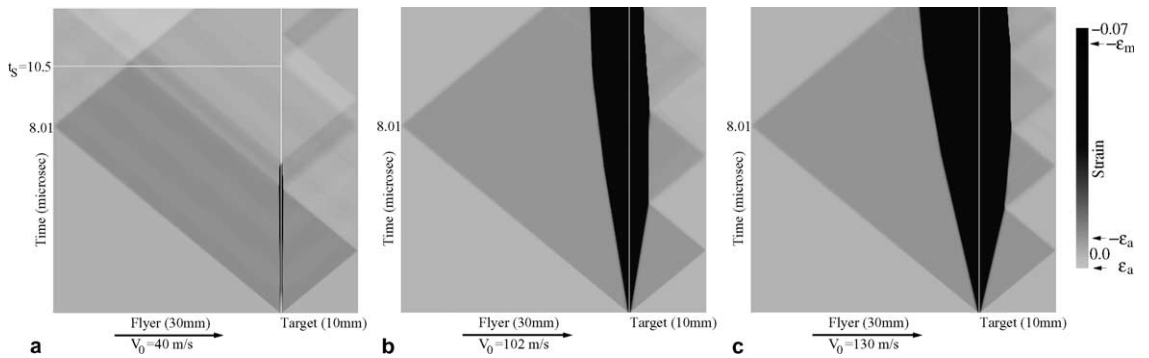

Fig. 7. Influence of the impact velocity on the interaction between the phase boundary propagating in the flyer and the unloading waves reflected by the free end; $\mu = 9.5 \times 10^{-4}$ MPa s.

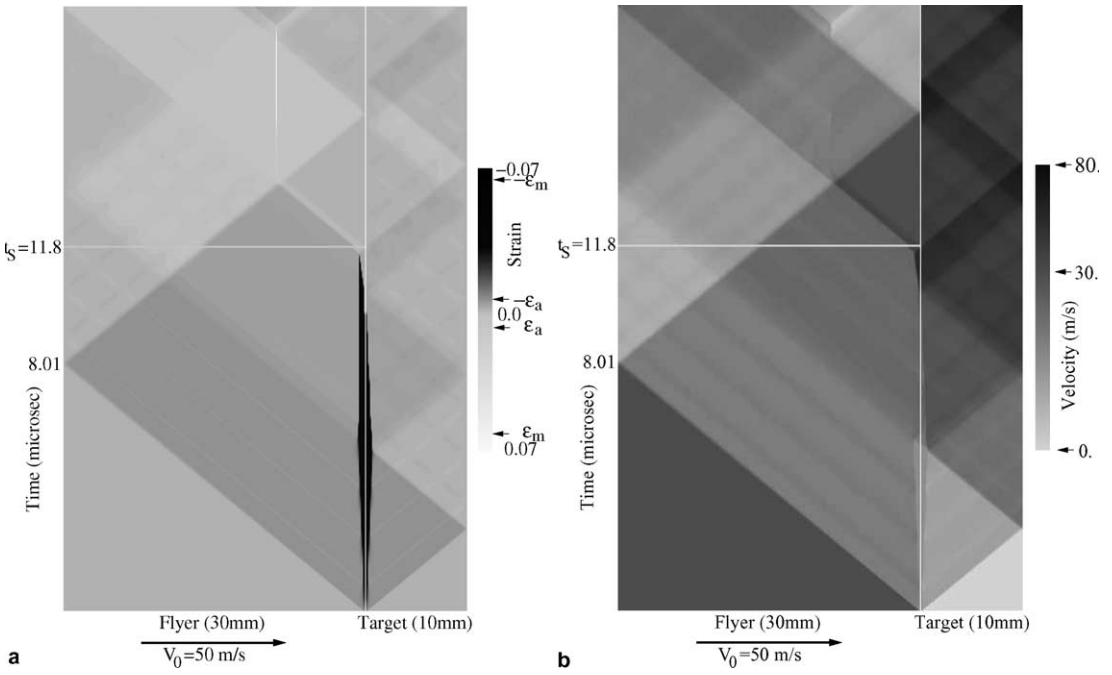

Fig. 8. Strain and velocity distribution in the bars after a moderate impact; $\mu = 9.5 \times 10^{-4}$ MPa s.

Another prediction in the frame of the elastic bar theory concerns the velocity level of the first peak. This characteristic value of a phase transformation in the flyer is $V_{ch} = V_{ph} + 2\sigma_m\sigma_3/(4\sigma_m + \sigma_3)/\sqrt{\varrho E_1} = 57.5$ m/s. We also recover this result for the rate-type model with the following differences (see Fig. 6a). For the rate-type model, if the impact velocity is only slightly larger then V_{ph} the transformation could be not complete, that is the particles at the impact face enter in the spinodal region but return quickly in the austenitic phase. In this case, a change in impedance still appears near the impact face and the elastic pulse is reflected near the contact point after a round trip in the target. In this case we get at the free-end of the target a slightly and periodically increase of the velocity, but at a level much lower then V_{ch} predicted by the elastic model (see Fig. 6a).

Another peculiarity of the rate-type model concerns the appearance of some oscillations of the particle velocity between the first arrival of the loading wave and until the arrival of the second loading wave (Fig. 6). These oscillations are in fact manifestations at the target free-end of some stress waves which appear just after the impact and propagates inside the transformed zone, being reflected and transmitted across the phase boundaries. These stress waves will be analyzed later in connection with Fig. 9. Let us note that the existence of such oscillations for the target free-end velocity instead of a plateau, was obtained by Escobar and Clifton (1995) for the normal and transverse particle velocity in a shear-plate impact experiment.

By increasing now the impact velocity the transformed region increases and the separation time changes. As long as a phase boundary is still present near the impact face, each elastic pulse reflected by the free-end of the target interacts as an unloading wave with the transformed zone being reflected as a loading wave. This produces each time a new step-like increase of the particle velocity at the monitoring surface (see Fig. 6b for velocities higher than 40 m/s). It is obvious that the time intervals between the velocity pulses can be related to the thickness of the evolving transformed region.

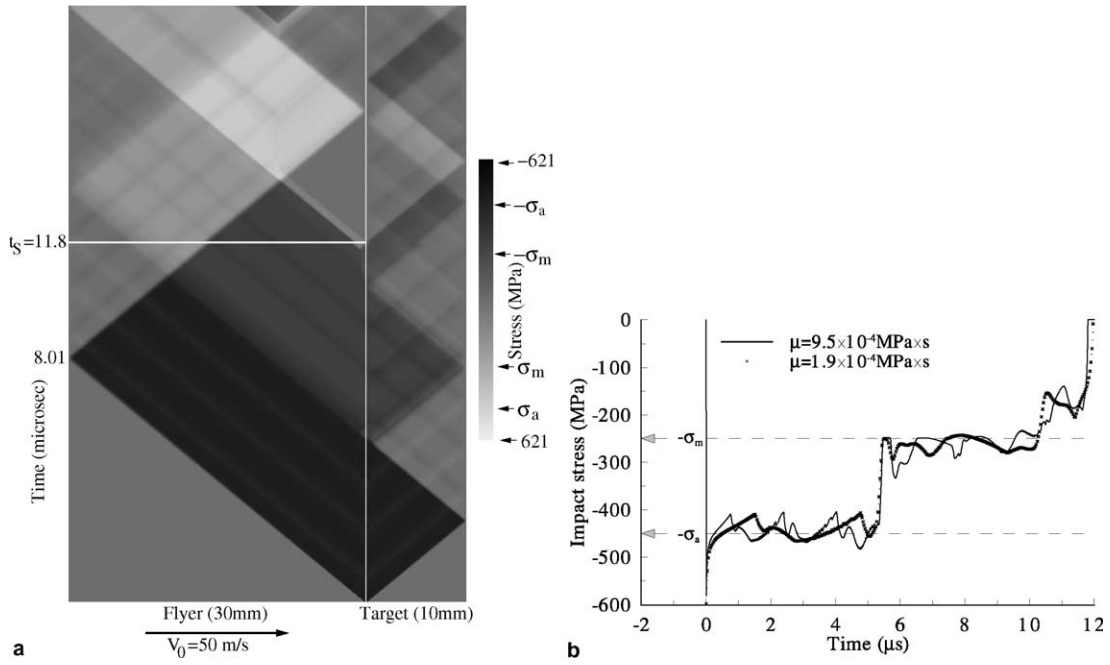

Fig. 9. Stress distribution in the bars after a moderate impact and the corresponding stress-impact history $\sigma(0,t)$.

We also investigate numerically the interaction between the first unloading wave with the propagating phase boundary. Critical values of the impact velocity V_0 have been determined in the elastic case such that this phase boundary after interaction propagates backward, remains stationary or propagates forward. Thus, if $V_0 \in (V_{\rm ph} = 37.2\ \text{m/s},\ V_{\rm bw} = 75.4\ \text{m/s})$, where $V_{\rm bw} = V_{\rm ph} + 4\sigma_{\rm m}(\sigma_3 + 2\sigma_{\rm m})/(\sigma_3 + 4\sigma_{\rm m})/\sqrt{\varrho E_1}$, the phase boundary propagates backward. If $V_0 \in (V_{\rm bw} = 75.4\ \text{m/s}, V_{\rm fw} = 102.5\ \text{m/s})$, where $V_{\rm fw} = V_{\rm ph} + 4\sigma_{\rm a}(\sigma_3 + 2\sigma_{\rm a})/(\sigma_3 + 4\sigma_{\rm a})/\sqrt{\varrho E_1}$, the phase boundary remains stationary. If $V_0 > V_{\rm fw} = 102.5\ \text{m/s}$ then the phase boundary propagates forward. Figs. 7 and 8 illustrate that for the Maxwellian rate-type model this result is still verified.

By using the elastic bar theory we deduced that another indication of the appearance of a phase boundary at the impact face is a sudden change of the time of separation of the two bars. Indeed, if $V_0 \leqslant 37.2\,\text{m/s}$, numerical computations using the rate-type model predicts the separation between the two bars at time $t_{\rm S} = 15.85\ \mu\text{s} \in (\frac{2l}{C} = 15.69\ \mu\text{s},\ \frac{2l}{C_1} = 16.12\ \mu\text{s})$, i.e. after a round trip of the elastic wave in the flyer. When the critical value $V_{\rm ph}$ is slightly overcome a very thin transformed region is induced at the impact face and according to the elastic bar theory the time of separation drop to $t_{\rm S} = 4l/C_1$, that is the separation appears after two round trips of the elastic wave in the target. Our rate-type bar theory predicts the following time of separation: $t_{\rm S} = 10.67\mu\text{s}$ for $V_0 = 37.4\,\text{m/s}$, $t_{\rm S} = 10.68\ \mu\text{s}$ for $V_0 = 37.7\ \text{m/s}$ and $t_{\rm S} = 10.57\ \mu\text{s}$ for $V_0 = 40\ \text{m/s}$, values which lie in the interval $(4l/C = 10.46\ \mu\text{s},\ 4l/C_1 = 10.74\ \mu\text{s})$.

In general, for a moderate impact velocity like $V_0 = 50\ \text{m/s}$ the typical wave propagation picture is the following (see Fig. 8 and Fig. 9). The unloading wave reflected by the free end of the target interacts firstly with the phase boundary propagating forward in the flyer and transforms it in a backward propagating phase boundary. This elastic wave is reflected and transmitted across the phase boundary. The reflected wave travels through the target being successively reflected by the free-end of the target and the phase boundary propagating in the target each time reducing the speed of propagation of the phase boundary.

The transmitted elastic wave interacts with the phase boundary propagating in the flyer and stops it. Inside the transformed region elastic waves travel being reflected and transmitted successively by the two phase boundaries. The way these waves travel can be determined by analyzing the history of the particle velocity at the target free-end (see Fig. 6) and the history of the impact stress (see Fig. 9b). One of the most important events is the interaction between the two phase boundaries propagating in the flyer and in the target leading to the disappearance of the transformed zone. As it can be seen in Figs. 8 and 9 this interaction produces two tensile waves propagating right and left. When the right propagating tensile wave reaches the contact point it causes the separation of the two bars. For the impact velocity $V_0 = 50$ m/s the separation appears at $t_S = 11.8$ μs. It is interesting to note that after separation in the flyer a reverse transformation in the twin phase $\mathscr{M}^+$ may appear (see the strain distribution in Fig. 8 after t_S). This is produced by the interaction of two tensile waves. One is generated by the disappearance of the transformed zone $\mathscr{M}^-$ and the other is the unloading wave reflected by the free end of the flyer.

It is also useful to observe the behavior of the stress at the impact point (see Fig. 9b). According to the elastic model the stress should jump at $t = 0+$ at the value $\sigma_B(\eta) = -\sigma_a + \frac{\sigma_3}{2} - \frac{1}{2}\sqrt{\sigma_3^2 + \eta^2}$ where $\eta = \sqrt{\varrho E_1} V_0 - 2\sigma_a$ and remain constant until the unloading wave reflected by the target free-end reaches the contact point. If $V_0 = 50$ m/s this value is $\sigma_B = -454.2$ MPa. Since the rate-type model is characterized by a linear instantaneous response the compressive stress first jumps at the value $\sigma = -\sqrt{\varrho E} V_0 = -1242.$ MPa and after a few nanoseconds it decreases in absolute value at the level of the elastic plateau. Due to this rapid variation of the stress at the impact-end, elastic stress waves are generated inside the transformed zone leading to the oscillations on the first stress-plateau until the unloading wave transmitted across the phase boundary reaches the contact point and produces an abrupt increase of the stress at the level of $-\sigma_m = -250$ MPa. This peculiar behavior of the instantaneous rate-type model is also responsible on the oscillations of the target free-end particle velocity already remarked in Fig. 6. and make a difference between the two studied models. Let us note that the amplitude of the oscillations around the elastic plateau depends on the viscosity coefficients μ too, i.e. on the kinetics of the phase transformation (see Fig. 9b). On the other side, the oscillations of the stress which appear at the level of $-\sigma_m = -250$ MPa reflects the effect of the stress waves propagating inside the transformed zone before the reverse transformation starts and are described by both models. Their presence can be also related with the small oscillations observed on the graph of the target free-end particle velocity (see Fig. 6). The arrival at the contact point of the second unloading wave leads to a new increase of the stress above the value $-\sigma_m = -250$ MPa (Fig. 9b) and indicates the beginning of the reverse transformation in the target. The impact stress oscillates again several times before increasing sharply at zero stress which corresponds with the time of separation between the two bars.

Finally, in order to test the theoretical results established previously and the capability of the numerical scheme used we illustrate in Fig. 10 the influence of the viscosity coefficient μ on the particle velocity $v(l, t)$ for large time behavior. We observe how the amplitude of the velocity peaks decays after each round trip propagation of the elastic wave in the flyer. It is obvious that for large μ the decay of the amplitude is more important which is in agreement with the results obtained in Section 5 concerning the propagation of delayed waves. There, we have shown that in a pure phase the disturbances spreads out *for large t* like $\sqrt{at}$, while their amplitude decreases like $1/\sqrt{at}$ where a is a diffusion coefficient given by (89). Therefore, the diffusion process becomes more important for a large viscosity coefficient μ. Indeed the dash lines in Fig. 10 show that the amplitude of the velocity peaks decreases like $V_0 + \frac{b}{\sqrt{a(t-t_0)}}$, where $a = 0.003846$ m^2/s for $\mu = 9.5 \times 10^{-4}$ MPa s and $a = 0.03846$ m^2/s for $\mu = 9.5 \times 10^{-3}$ MPa s while b and t_0 are appropriate constants, i.e., $b = 75486$ mm^2/s and $t_0 = -441.688$ μs, respectively $b = 9809.97$ mm^2/s and $t_0 = -21.59$ μs. This result also shows that for the viscosity coefficient $\mu = 9.5 \times 10^{-4}$ MPa s, mainly used in our numerical applications, the diffusive aspects are less important. Another way to eliminate completely the diffusion of the wave motion is to choose in our input data $E = E_1 = E_3 = 90$ GPa.

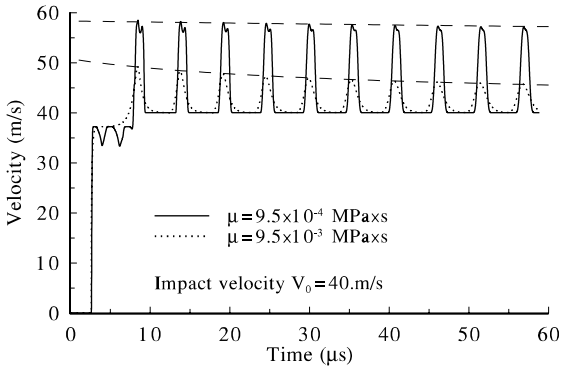

Fig. 10. Influence of the Newtonian viscosity μ on the free-end velocity of the target $v(l,t)$. Dash lines illustrate the amplitude decrease of the velocity peaks like $V_0 + b/\sqrt{a(t-t_0)}$, where a is the diffusion coefficient (89).

7. Summary and concluding remarks

We investigated the potentiality of the Maxwellian rate-type model, with a non-monotone equilibrium stress–strain relation, to describe specific phenomena accompanying phase transformations induced by longitudinal impact of thin bars. Such simple tests have been considered since they are reproducible in laboratory experiments and provide insight into the kinetics of phase transformation.

We showed that for describing phase transition phenomena there are some advantages from physical and mathematical point of view in using the Maxwell rate-type model instead of the Kelvin–Voigt model, or of the elastic model equipped with the viscosity criterion. We illustrated that this so called "viscoelastic" constitutive equation should be seen as a "kinetic law" for transformation between low strain and high strain phases and we emphasized the role of the material parameters in the nucleation and growth processes. The viscosity coefficient, which plays a major role in the kinetics of phase transformation, may depend on strain, that is it may be different for different phases of the material. In the simplest case, when the rate sensitivity parameter $\lambda = 1$, the growth factor in the unstable phase and the damping factor in the stable phase are characterized by the ratio between the slope of the elastic curve and the viscosity coefficient. These quantities, which are responsible of the kinetics of phases, should be connected with information coming from nucleation theory in phase transition like the time of nucleation or time of growth of microscopic theories (Christian, 1975). The Maxwellian rate-type approach leads to a *hyperbolic* semilinear system in both stable and unstable phases and consequently it is appropriate to describe the propagation of disturbances. We proved that the general form of the proposed rate-type constitutive equation associates, like the Kelvin–Voigt model, to the corresponding elastic system the chord criterion as admissibility criterion for sharp phase boundaries. We investigated systematically for both rate-type and elastic systems the *dissipation* induced by smooth or sharp strain discontinuities. Thus, it was shown that the total internal dissipation induced by a traveling wave which describes a smooth phase boundary in the rate-type theory is just the dissipation induced by a sharp phase boundary in the elastic theory. It was also seen that the instantaneous waves of the Maxwellian rate-type system can describe *the nucleation and growth of phases* in the spinodal region. Although the rate-type terms may introduce a diffusion effect in the wave motion, according to our analysis, this can be avoided by taking the dynamic Young modulus very close or even equal to the elastic modulus of the stable phase. In this last case there is no diffusivity even the viscosity coefficient is strictly positive. Moreover, the instantaneous and delayed waves coincide.

If one compares the Maxwellian rate-type approach with the Kelvin–Voigt approach the main difference arises from the type of the system. Kelvin–Voigt viscous regularization system is of *parabolic* type and

therefore it is not appropriate for describing propagation of disturbances with finite speed. Moreover, in this case inherent diffusivity aspects of the solution can be eliminated only in a limit of vanishing viscosity.

If one compares the Maxwellian rate-type approach with the elastic non-monotone system equipped with the chord criterion we get, specially for small values of the viscosity coefficient, a very good agreement between the predictions of the two models. Thus, numerical simulations were conducted using input data appropriate for a NiTi shape memory alloy and the similitude and differences between the predictions of the two models have been analyzed. The influence of the impact velocity and kinetic parameters on measurable quantities like the time of separation between the bars, velocity profile at the free end of the target and stress history at the impact point were analyzed since these information are useful to interpret laboratory measurements. It is also useful to note that while the Maxwellian rate-type model can be successfully used in quasistatic experiments (Făciu and Suliciu, 1994; Făciu, 1996) the elastic model in this form is insufficient.

Acknowledgements

A.M. acknowledge partial support of the EURROMMAT Programme ICA1-CT 2000-70022 of the European Commission. C.F. acknowledge support from the Romanian Ministry of Education and Research (CNCSIS Programme Project 33079/2004).

References

Bell, J.F., 1968. The Experimental Foundations of Solid MechanicsHandbuch der Physik, vol. VIa/1. Springer-Verlag, Berlin–Heidelberg–New York.

Brun, L., Molinari, A., 1982. Transient linear and weakly non-linear viscoelastic waves. In: Mainardi, F. (Ed.), Wave Propagation in Viscoelastic Media. Research Notes in Mathematics, vol. 52. Pitman, pp. 65–94.

Christian, J.W., 1975. The Theory of Transformations in Metals and Alloys: Part I. Pergamon Press, Oxford.

Cristescu, N., Suliciu, I., 1982. Viscoplasticity. Martinus Nijhoff Publishers, The Hague/Boston/London.

Escobar, J.C., Clifton, R.J., 1995. Stress-wave induced martensitic phase transformations. In: Murr, L.E., Staudhammer, K.P., Meyers, M.A. (Eds.), Metallurgical and Materials Applications of Shock-Wave and High-Strain-Rate Phenomena. Elsevier Science B.V., pp. 451–462.

Făciu, C., 1991. Numerical aspects in modelling phase transitions by rate-type constitutive equations. Int. J. Eng. Sci. 29, 1103–1119.

Făciu, C., 1996. Initiation and growth of strain bands in rate-type viscoelastic materials. Part I: Discontinuous strain solutions. Part II: The energetics of the banding mechanism. Euro. J. Mech. A/Solids 15, 969–988, 989–1011.

Făciu, C., Mihăilescu-Suliciu, M., 1987. The energy in one dimensional rate-type semilinear viscoelasticity. Int. J. Solids Struct. 11, 1505–1520.

Făciu, C., Mihăilescu-Suliciu, M., 2002. On modelling phase propagation in SMAs by a Maxwellian thermo-viscoelastic approach. Int. J. Solids Struct. 39, 3811–3830.

Făciu, C., Molinari, A., 2005. On the longitudinal impact of two phase transforming bars. Elastic versus a rate-type approach. Part I: The elastic case. Int. J. Solids Struct., in press, doi:10.1016/j.ijsolstr.2005.06.023.

Făciu, C., Suliciu, I., 1994. A Maxwellian model for pseudoelastic materials. Scrip. Metall. Mater. 31, 1399–1404.

James, R.D., 1980. The propagation of phase boundaries in elastic bars. Arch. Rat. Mech. Anal. 73, 125–158.

Jeffrey, A., Taniuti, T., 1964. Nonlinear Wave Propagation. Academic Press.

Kukudjanov, V.N., 1967. Propagation of elasto-plastic waves in rods taking into account the rate influence. Comput. Centr. Acad. Sci. USSR 6.

Mihăilescu-Suliciu, M., Suliciu, I., 1992. On the method of characteristics in rate-type viscoelasticity with non-monotone equilibrium curve. Z. Angew. Math. Mech. 72, 667–674.

Nayfeh, A., 1973. Perturbation Methods. John Wiley Publ.

Ngan, S.-C., Truskinovsky, L., 2002. Thermo-elastic aspects of dynamic nucleation. J. Mech. Phys. Solids 50, 1193–1229.

Pego, R.L., 1987. Phase transitions in one-dimensional nonlinear viscoelasticity: admissibility and stability. Arch. Rat. Mech. Anal. 97, 353–394.

Shaw, J.A., Kyriakides, S., 1997. On the nucleation and propagation of phase transformation fronts in a NiTi alloy. Acta Mater. 45, 683–700.

Slemrod, M., 1983. Admissibility criteria for propagating phase boundaries in a van der Waals fluid. Arch. Rat. Mech. Anal. 81, 301–315.

Suliciu, I., 1990. On modeling phase transitions by means of rate-type constitutive equations. Shock wave structure. Int. J. Eng. Sci. 28, 829–841.

Suliciu, I., 1992. Some stability–instability problems in phase transitions modeled by piecewise linear elastic or viscoelastic constitutive equations. Int. J. Eng. Sci. 30, 483–494.

Suliciu, I., Malvern, L.E., Cristescu, N., 1972. Remarks concerning the plateau in dynamic plasticity. Arch. Mech. 24, 99–1011.

Vainchtein, A., 2002. Dynamics of non-isothermal martensitic phase transitions and hysteresis. Int. J. Solids Struct. 39, 3387–3408.

Vainchtein, A., Rosakis, P., 1999. Hysteresis and stick-slip motion of phase boundaries in dynamic models of phase transitions. J. Nonlin. Sci. 9, 697–719.

Whitham, G.B., 1959. Some comments on wave propagation and shock wave structure with applications to magnetohydrodynamics. Commun. Pure Appl. Math. 12, 113–158.